Templated Electrochemical Deposition of Nanostructured Materials and their Applications.

P. N. Bartlett

University of Southampton

Report Documentation Page

Form Approved
OMB No. 0704-0188

1. REPORT DATE	2. REPORT TYPE	3. DATES COVERED
00 JUN 2003	**N/A**	**-**

4. TITLE AND SUBTITLE	5a. CONTRACT NUMBER
Templated Electrochemical Deposition of Nanostructured Materials and their Applications	5b. GRANT NUMBER
	5c. PROGRAM ELEMENT NUMBER
6. AUTHOR(S)	5d. PROJECT NUMBER
	5e. TASK NUMBER
	5f. WORK UNIT NUMBER
7. PERFORMING ORGANIZATION NAME(S) AND ADDRESS(ES) **University of Southampton**	8. PERFORMING ORGANIZATION REPORT NUMBER
9. SPONSORING/MONITORING AGENCY NAME(S) AND ADDRESS(ES)	10. SPONSOR/MONITOR'S ACRONYM(S)
	11. SPONSOR/MONITOR'S REPORT NUMBER(S)

12. DISTRIBUTION/AVAILABILITY STATEMENT
Approved for public release, distribution unlimited

13. SUPPLEMENTARY NOTES
See also ADM001697, ARO-44924.1-EG-CF, International Conference on Intelligent Materials (5th) (Smart Systems & Nanotechnology)., The original document contains color images.

14. ABSTRACT

15. SUBJECT TERMS

16. SECURITY CLASSIFICATION OF:			17. LIMITATION OF ABSTRACT	18. NUMBER OF PAGES	19a. NAME OF RESPONSIBLE PERSON
a. REPORT	b. ABSTRACT	c. THIS PAGE			
unclassified	**unclassified**	**unclassified**	**UU**	**46**	

Electrodeposition

- $M^{n+}(aq) + n\mathbf{e} \rightarrow M(s)$
- $M(aq) \rightarrow (M)_n + 2n\mathbf{e}$
- Control over rate/amount/thickness
  - *E*, *i*, *Q* and *t*
- Control over composition
- Coatings on conducting substrates
- Coatings on patterned substrates
- Thin films, large areas, membranes

Electrodeposition

- Metals
  - Pt, Pd, Ni, Au, Ag, Cu,…
  - more reactive metals (Sn, Zn,…)
  - alloys
- Oxides
  - Cu_2O, ZnO, PbO_2, WO_3,....
- Polymers
  - conducting polymers (pyrrole, aniline,…)
  - insulating polymers (phenol, diaminobenzene,...)

The Driving Force for Electron Transfer

Electron transfer is an event on a molecular scale.

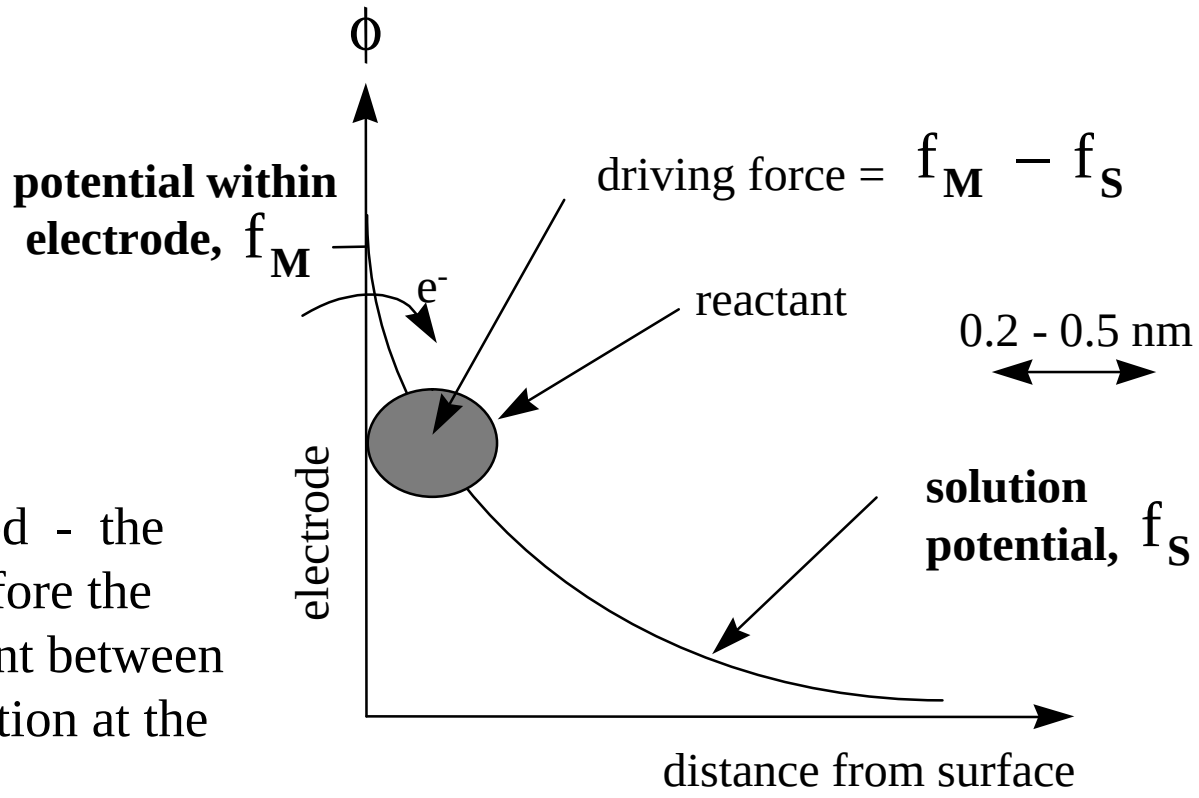

The electron is charged - the driving force is therefore the local potential gradient between the electrode and solution at the interface.

The required potential difference also depends on the molecular structures of the reactant/product

The potential distribution at the electrode electrolyte interface is determined by the balance of coulombic forces between the ions and the electrode and random thermal motion. For concentrated electrolyte solutions (e.g. 0.1 M) most of the potential is dropped in a thin layer one ion thick at the electrode surface (the Helmholtz layer) with the diffuse layer making up the rest.

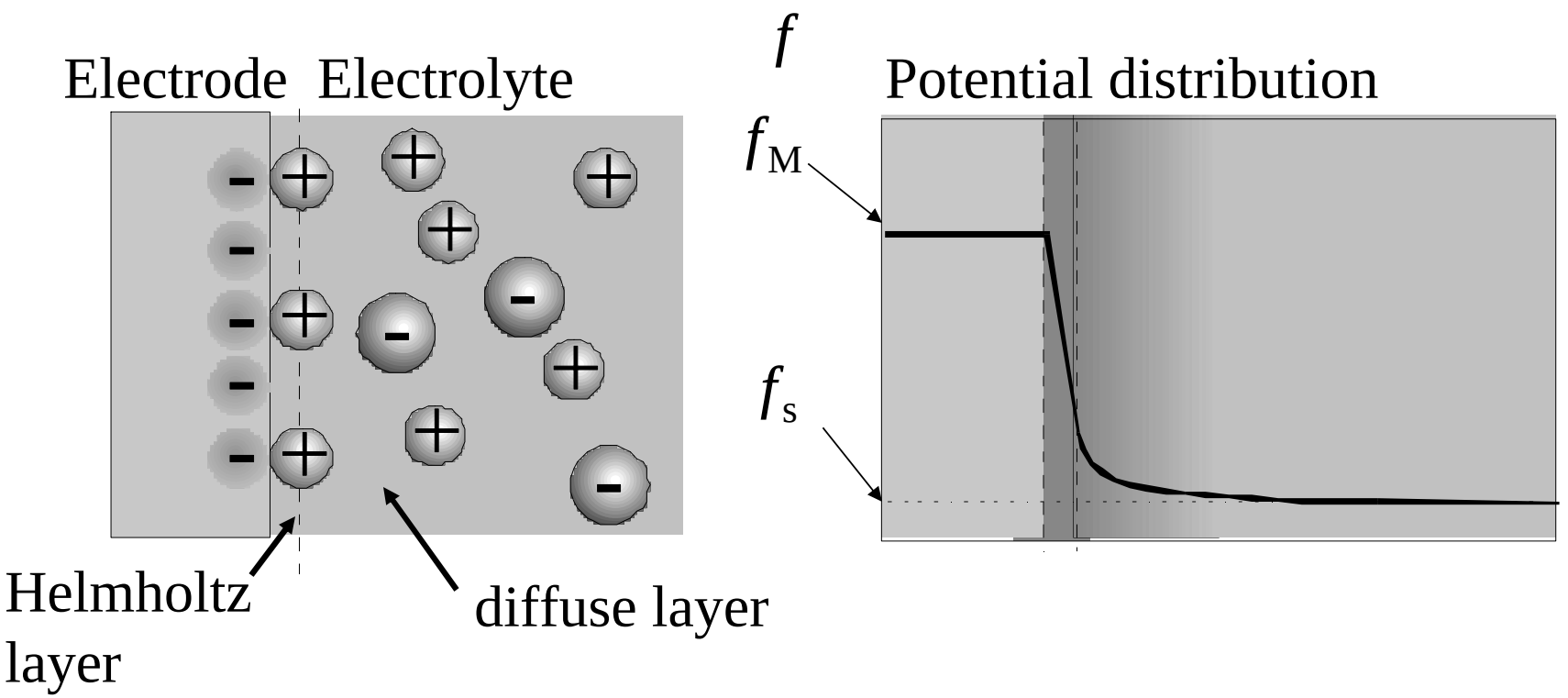

The Potential Distribution

When you change the potential of the electrode you change the charge on the electrode and the distribution of ions in solution close to/at the electrode surface:

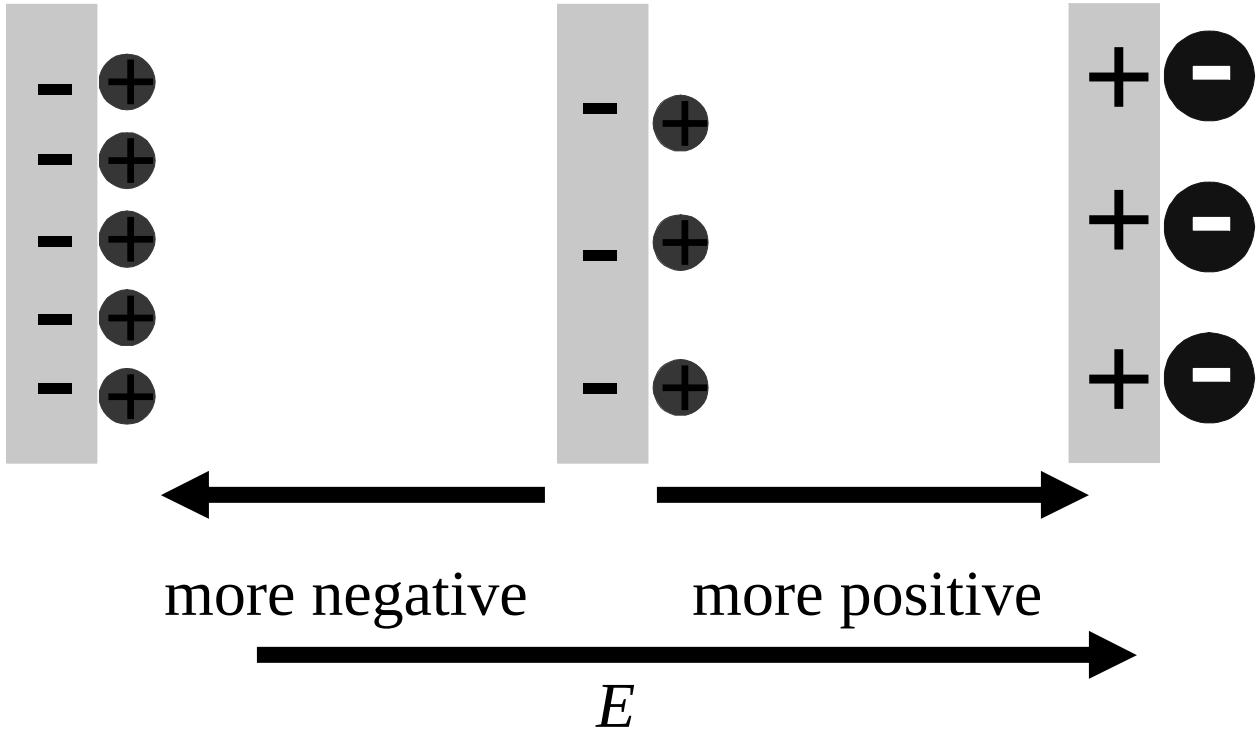

the electrode behaves like a capacitor

Electron Transfer and Equilibrium

The current flowing is directly related to the **net** rate of electron transfer

$$I = nFj$$

where I is the current density, n the number of electrons transferred, F the Faraday (96480 C mol^{-1}) and j is the net flux (mol cm^{-2} s^{-1}).

At the equilibrium potential no net current flows because the rates of forward and backward reactions are exactly in balance.

$$M^{z+}(solution) + ze^- \rightleftharpoons M(s)$$

$$j = \overleftarrow{j} + \overrightarrow{j} = 0$$

Equilbrium is a dynamic situation.

The position of equilibrium (i.e. where $I = 0$) is given by the Nernst Equation

$$E_e = E_e^o + \frac{RT}{nF} \ln \frac{a_O}{a_R}$$

where E_e^0 is the standard potential for the redox couple, R the gas constant (8.314 J K^{-1} mol^{-1}), F the Faraday (96480 C mol^{-1}), T the temperature, n the number of electrons transferred, and a_O and a_R the activities of the oxidised and reduced forms of the redox couple respectively. At 25 °C RT/F is 25 mV.

For metal deposition, neglecting activity effects in the solution, this can be approximated by

$$E_e = E_e^o + \frac{RT}{zF} \ln [M^{z+}]$$

where $[M^{z+}]$ is the concentration of the metal ion in solution and recognising that the activity of the pure metal is 1.

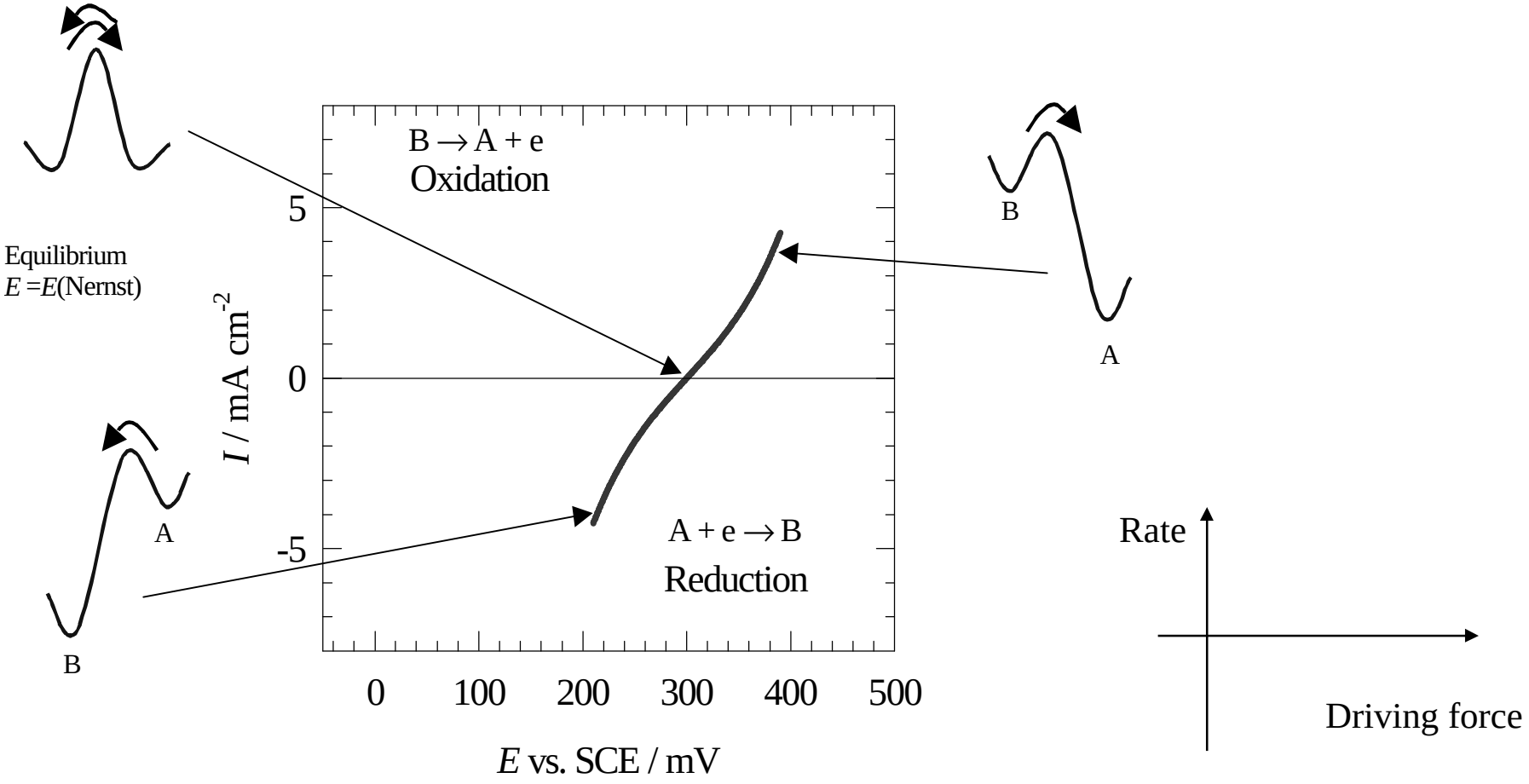

E is related to the **thermodynamic driving force** for the reaction

$$\Delta G = -nFE$$

I is a measure of the **rate of the reaction**

$$I = nFj$$

where *j* is the **flux** in mol cm^{-2} s^{-1}

Kinetics of Electron Transfer

The kinetics of electron transfer are described by the Butler Volmer equation

$$I = I_0 \left[\exp\left(\frac{a_A nF}{RT} h \right) - \exp\left(-\frac{a_C nF}{RT} h \right) \right]$$

where it has the form $I = \overleftarrow{I} + \vec{I}$. Usually $a_A = a_C = 0.5$ where a_A and a_C are the anodic and cathodic transfer coefficients, I_0 is the exchange current density and h is the overpotential ($h = E - E_e$)

At most potentials, either the anodic or cathodic partial current totally dominates. For example, at positive overpotentials $h > 100$ mV, the cathodic partial current density is negligible. Then

$$I = I_0 \exp \frac{a_A nF}{RT} h \quad \text{or} \quad \log I = \log I_0 + \frac{a_A nF}{2.3RT} h$$

This is the Tafel equation.

The electron transfer step is not the only step in the electrode reaction and it may not be the rate limiting step.

There can also be chemical steps whose rate is not driven by the electrode potential such as

$$ML_4 \rightarrow ML_3 + L$$

In addition mass transport of species from the solution bulk to the electrode surface may become rate limiting.

In general electrode reactions, and electrodeposition, involve a series a sequential reactions the slowest of which will determine the overall reaction rate and hence the overall current.

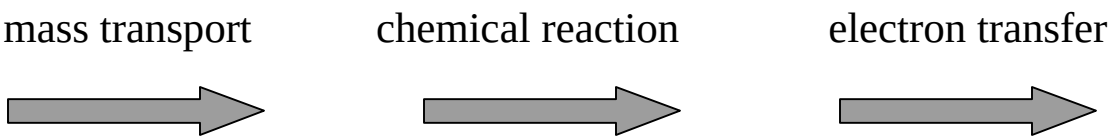

Nucleation and growth

Electrodeposition leads to the formation of a new phase deposited onto the electrode surface.

Consider the case of Cu deposition onto a C surface. The individual steps are:

1. Transport to the electrode surface
2. Electron transfer
3. Partial or complete desolvation
4. Surface diffusion
5. Formation of stable nucleus
6. Growth of nucleus

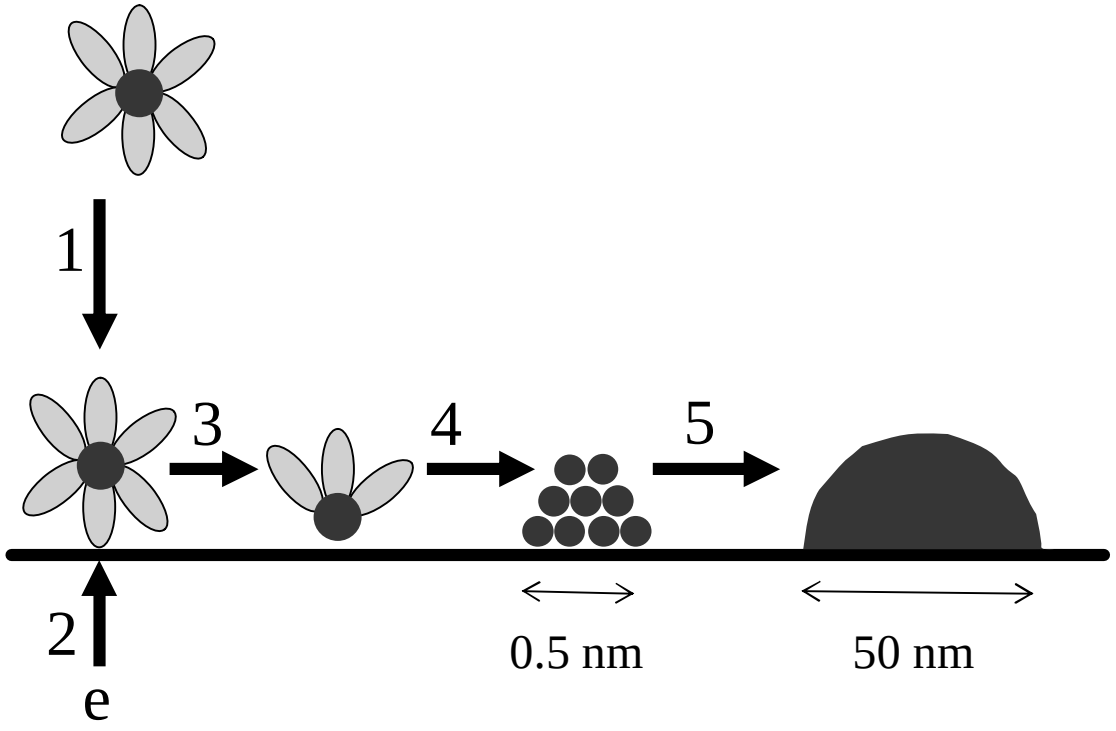

Growth of a large scale deposit proceeds in a number of stages:

clean surface

formation of 1st nucleus

further nucleation and growth

start of overlap

complete overlap

thickening

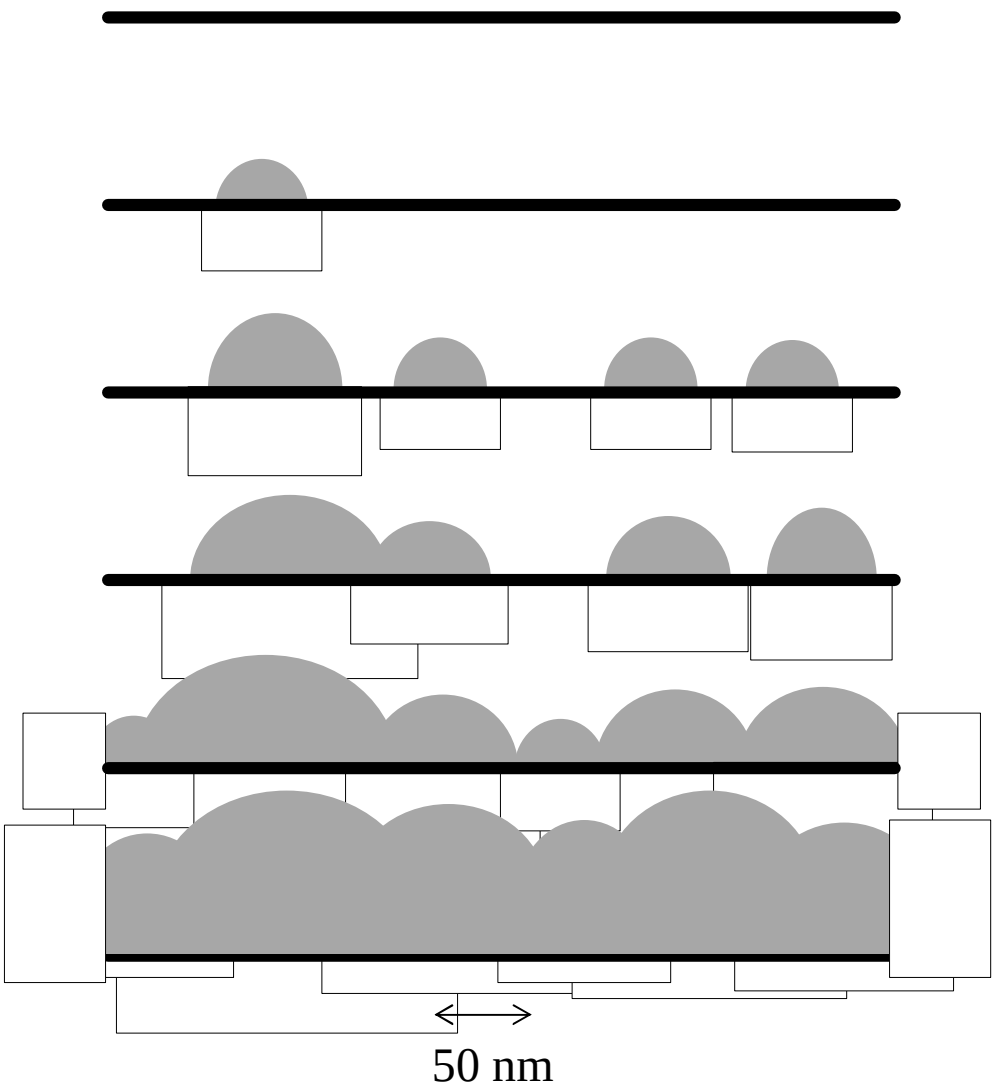

Metal Deposition

Example: deposition of Pd onto a vitreous carbon disc electrode from 10 mM $PdCl_2$ + 1 M KCl, pH 1.0, ν = 100 mV s^{-1}.

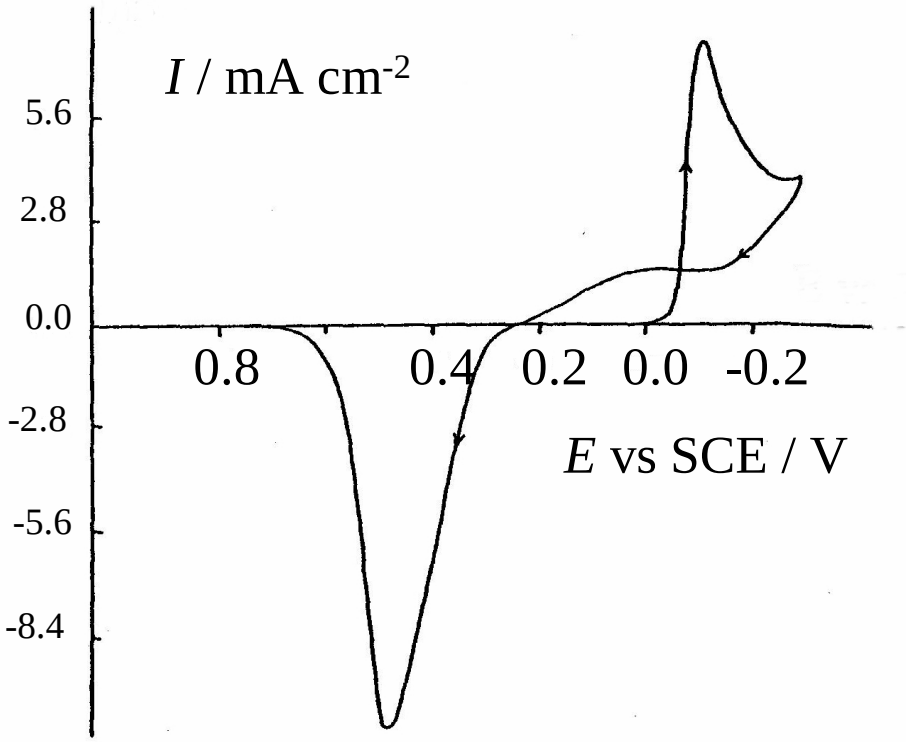

Note:

- Diffusion controlled reduction peak at -60 mV.
- The "nucleation loop" in the potential range -50 to +260 mV where metal deposition occurs on the reverse scan but j = 0 on the forward scan (due to the need for an overpotential to force nucleation).
- The symmetrical "anodic stripping peak" on the reverse scan at +450 mV (the shape is due to the finite amount of metal deposited).
- Charge balance: the anodic charge = the <u>total</u> cathodic charge.

Electroplating

In general

$$M^{n+}(aq) + n\mathbf{e} \rightarrow M(s)$$

where $M^{n+}(aq)$ is some suitable, soluble metal ion. Often the metal is complexed by some ligand (e.g. Cl^-, CN^-, acetate, etc.).

The choice of ligand (plating bath) has an important effect on the potential at which the deposition will occur, the rate of the metal deposition and the faradaic efficiency of the deposition.

Example of a plating bath for gold:

$KAu(CN)_2$ 40 g dm^{-3}

KH_2PO_4 100 g dm^{-3}

pH (KOH or H_3PO_4) 4.3-4.5

Gold is present as Au(I) in the form of the cyanide complex anion $[Au(CN)_2]^-$

Supporting electrolyte and pH control

There are often additives in the plating bath to improve the quality of the metal deposit

$$\text{Faradaic efficiency} = \frac{\text{Charge used to deposit metal}}{\text{Total charge passed}}$$

The Faradaic efficiency can be less than 100% because

- hydrogen is evolved along with metal deposition,
- some intermediate in the deposition escapes into bulk of solution,
- oxygen reduction occurs at the same time as metal deposition,
- etc.

In electroplating

- start/stop the process by controlling the potential, E
- we can control the rate of the metal deposition through choice of h, mass transport (stirring), concentration of metal ions, kinetics of associated chemical reactions
- we can control the amount of material deposited (thickness of metal) by controlling the charge passed (need to know the faradaic efficiency).

$$Q = \int i \, \mathrm{d}t = nmF \qquad \text{Faraday's law}$$

Electrochemical Polymerisation of Aniline

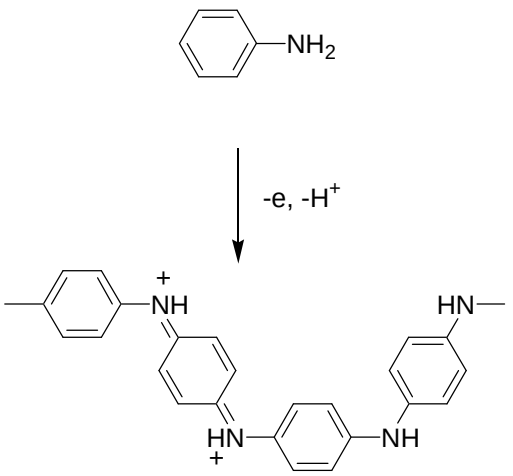

As more polymer is deposited with each cycle the peaks at 0.2 and 0.0 V for oxidation and reduction of the film grow in size.

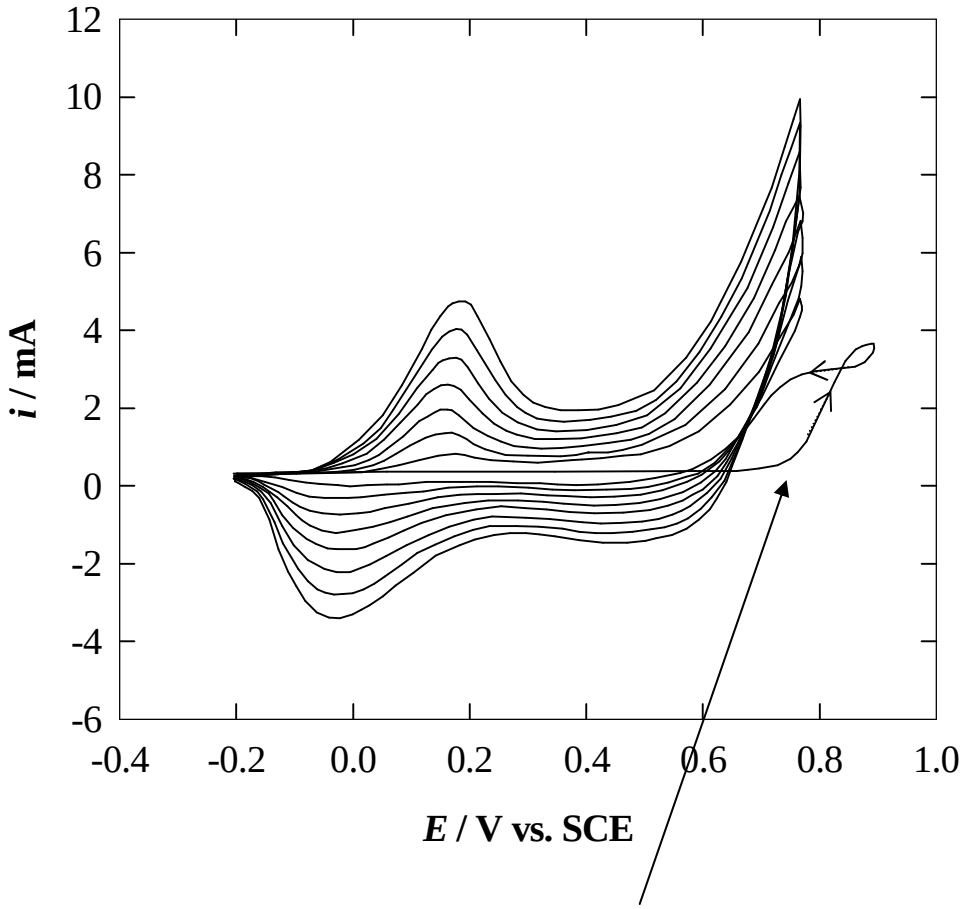

nucleation loop on first cycle

0.5 M aniline, 1 M HCl, glassy carbon electrode (area 0.38 cm^2) sweep rate 50 mV s^{-1}.

Nanostructures

Top-down approach

lithography
mechanical milling
precision engineering

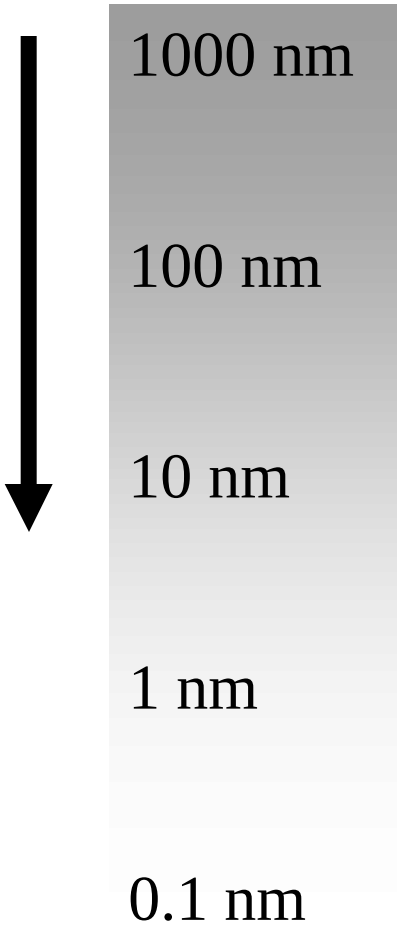

self-assembly
templating
precipitation

Bottom-up approach

Why make nanostructured materials?

Mesoscale nanoarchitecture

(match feature size to coherence length)

Introducing regular nanoarchitectures on the 1-1000 nm scale alters the physical properties of materials

- Effects of optical properties

  photonic crystals, photonic mirrors

- Effects on magnetic properties
- Effects on superconducting properties
- High surface area (catalysis)
- Thin walls (rapid insertion reactions)
- Free volume for expansion

Templated Electrodeposition

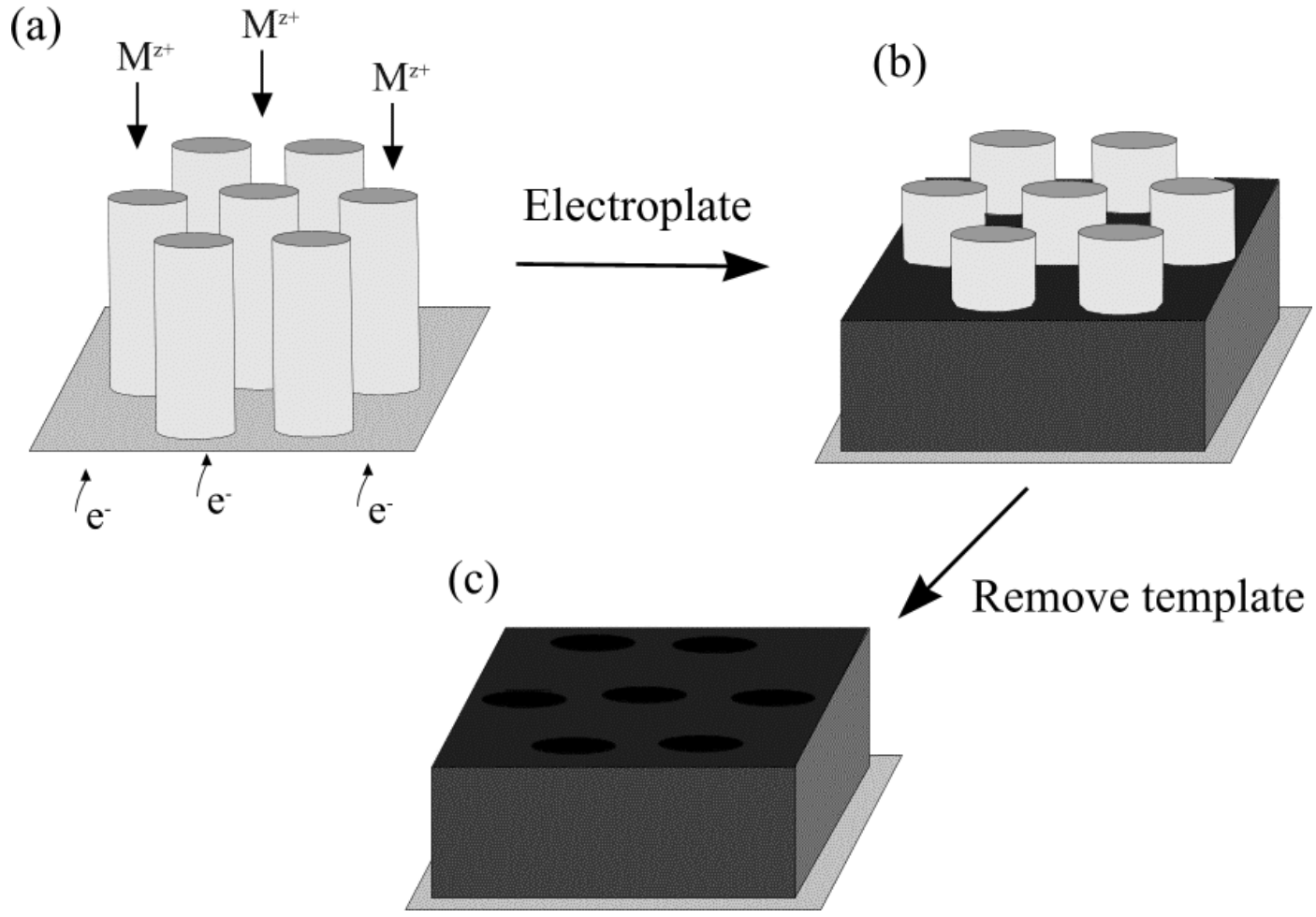

G. S. Attard, P. N. Bartlett, N. R. B. Coleman, J. M. Elliott, J. R. Owen, and J. H. Wang, "Nanostructured platinum films from lyotropic liquid crystalline phases", *Science*, **278**(1997)838-840.

Non-ionic Surfactants

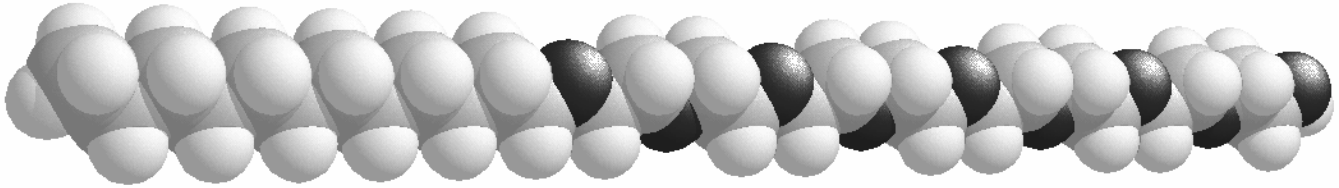

Octaethylene glycol monododecyl ether ($C_{12}EO_8$)

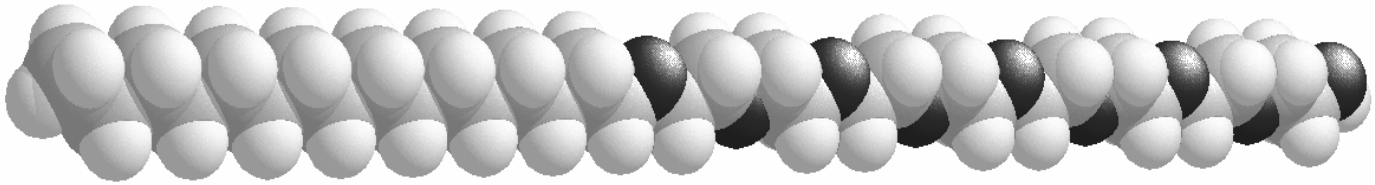

Octaethylene glycol monohexadecyl ether ($C_{16}EO_8$)

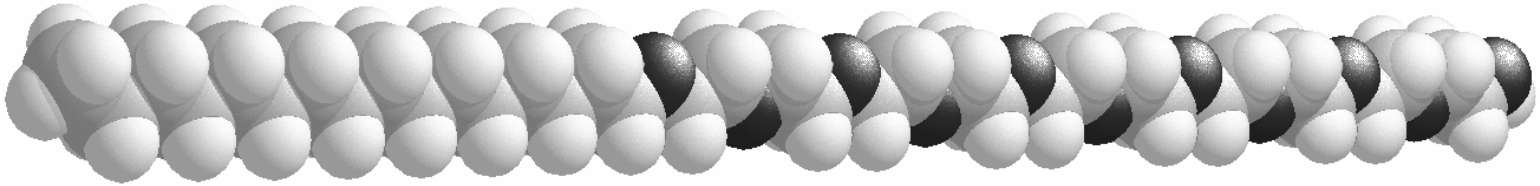

Polyoxyethylene(10) cetyl ether (Brij® 56)

Phase diagram

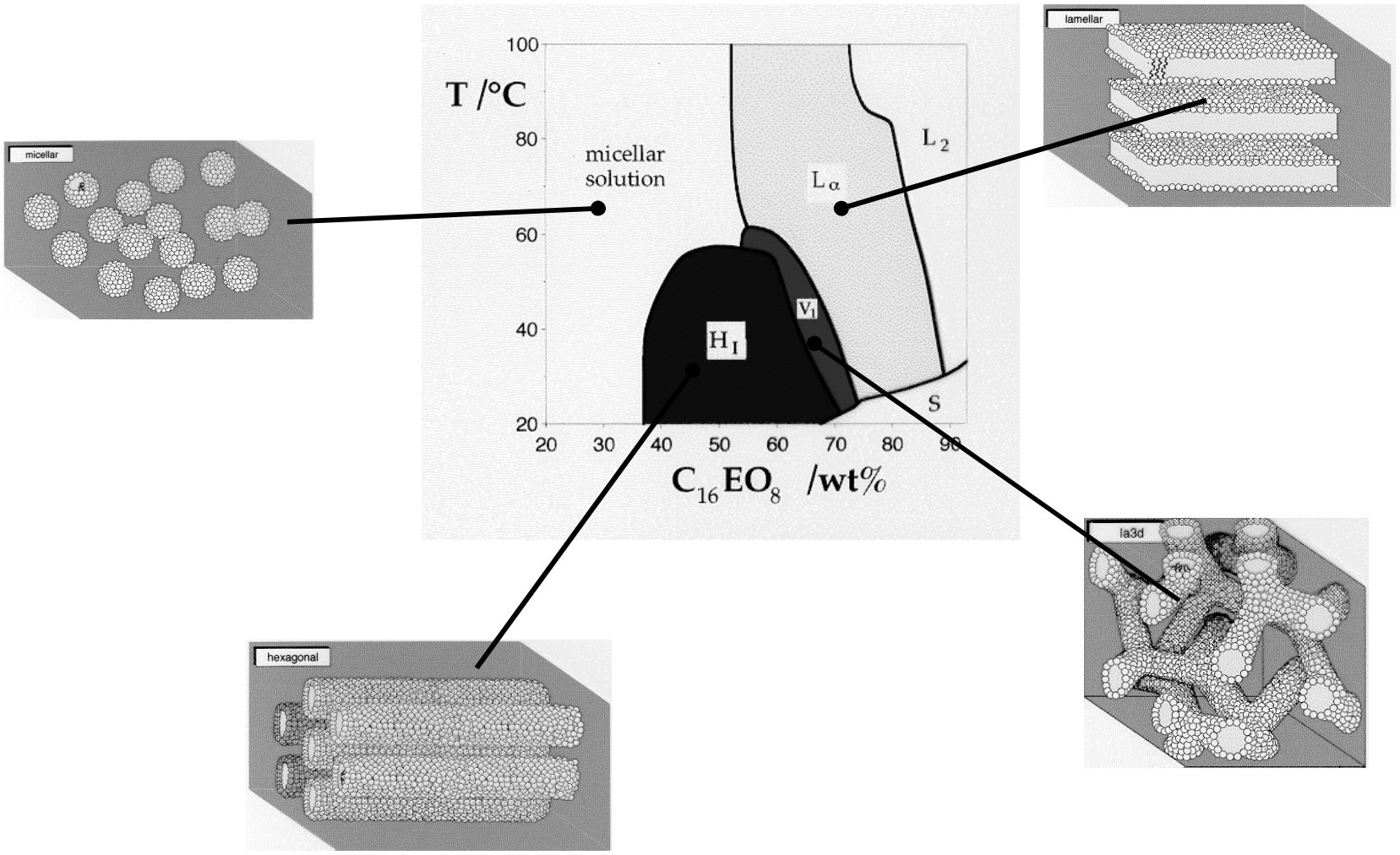

G. S. Attard, P. N. Bartlett, N. R. B. Coleman, J. M. Elliott, and J. R. Owen, “Lyotropic liquid crystalline properties of nonionic surfactant/H_2O/hexachloroplatinic acid ternary mixtures used for the production of nanostructured platinum”, *Langmuir*, **14**, 1998, 7340-7342.

H_I-ePt Deposition

- Deposition
  - 42% octaethyleneglycol monohexadecyl ether ($C_{16}EO_8$)
  - 29% H_2PtCl_6
  - 29% water
  - 25 - 65 ° C
  - -0.1 V vs SCE

- After deposition
  - remove surfactant by washing with water

Electrochemistry:

$$[Pt(Cl)_6]^{2-} + 2e \rightarrow 2Cl^- + [Pt(Cl)_4]^{2-}$$

Intermediate Pt^{II} d^8
square planar

Pt^{IV} d^6
octahedral

loss to solution
bulk

$$[Pt(Cl)_4]^{2-} + 2e \rightarrow 4Cl^- + Pt$$

Faradaic efficiency < 100%

complex mechanism of electron transfer steps and chemical steps

Nanostructured Pt Films

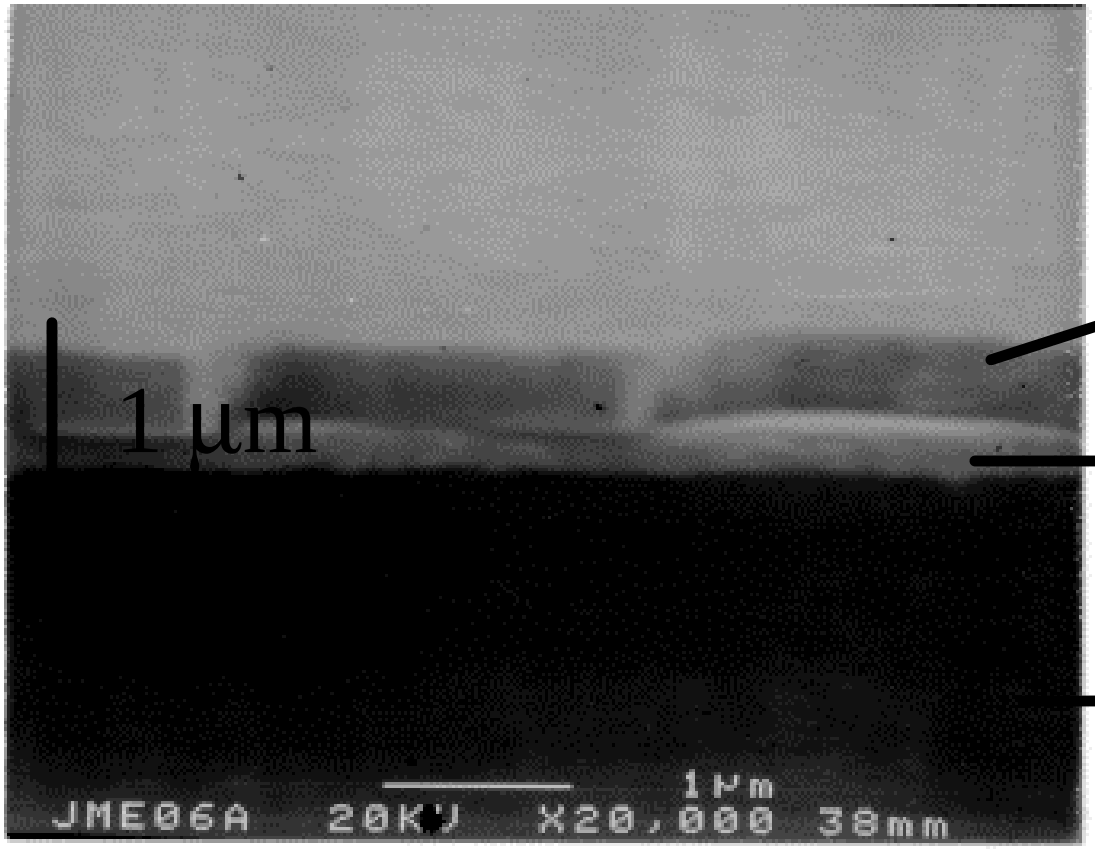

H_l-ePt

Au

Glass

H_I-ePt TEM

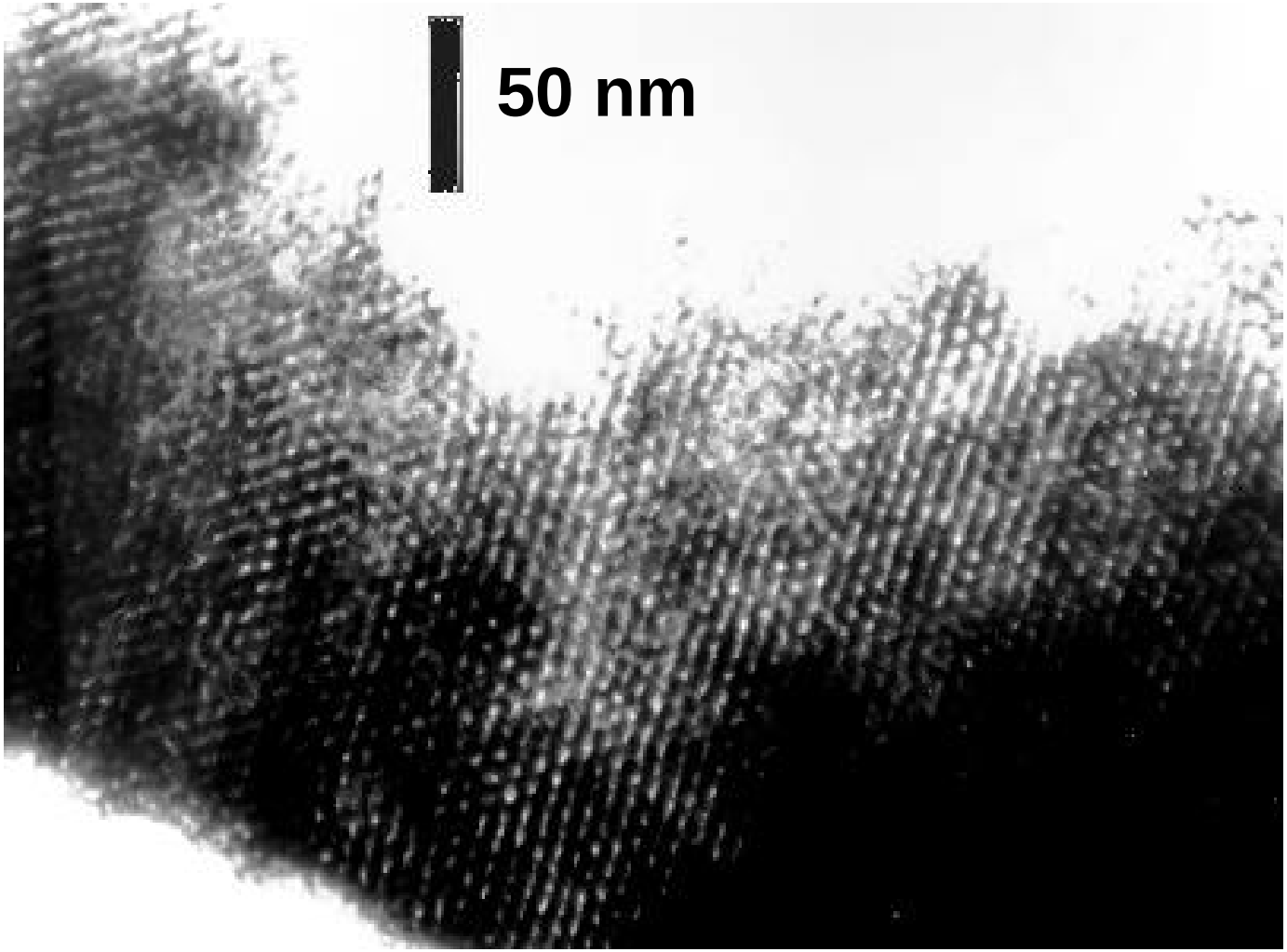

Deposited from: $C_{16}EO_8$: heptane 1:1

H_I-ePt TEM

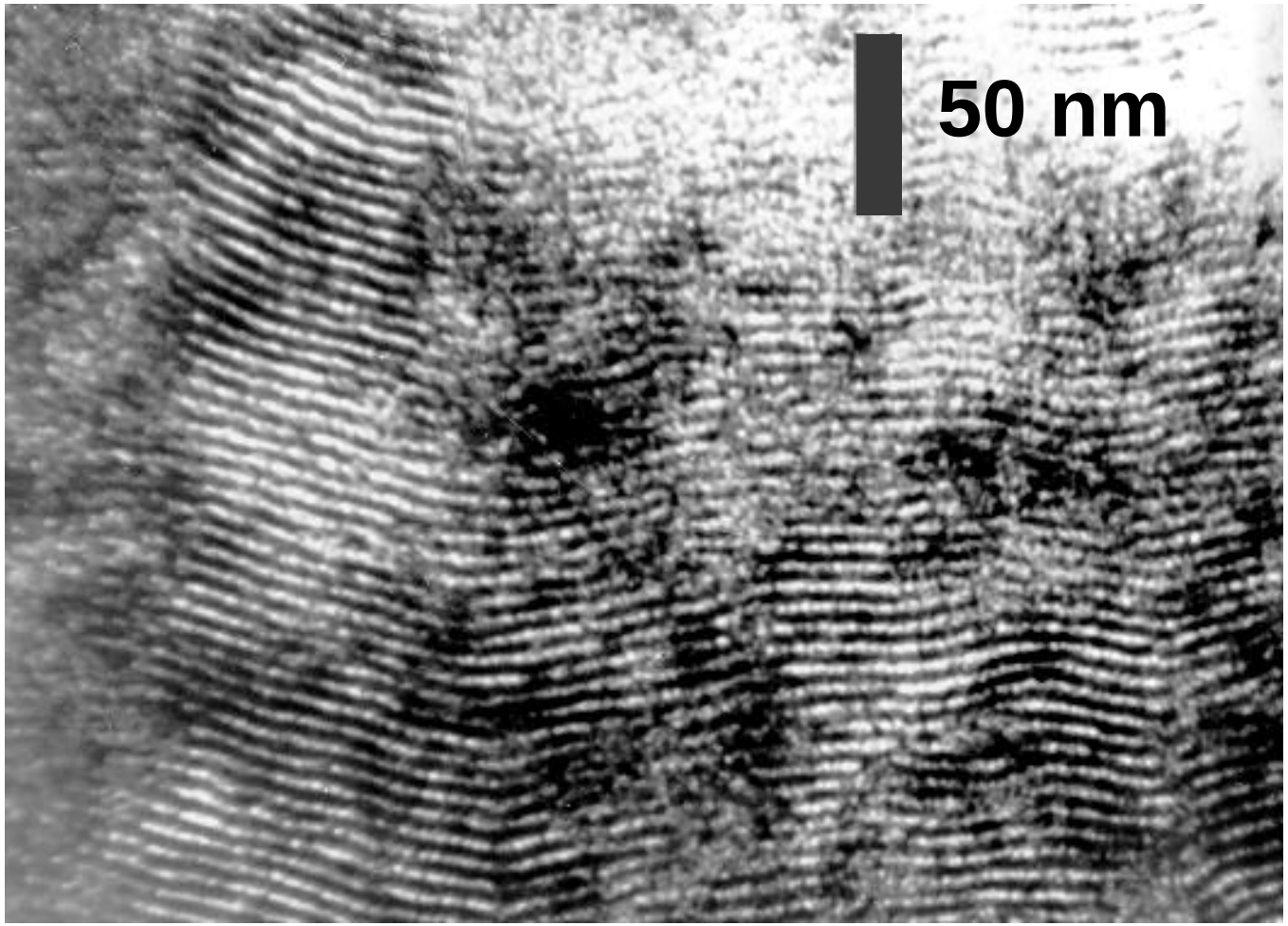

Deposited from: $C_{16}EO_8$: heptane 1:1

Pt Cyclic voltammetry

Compare to polycrystalline Pt

Use charge (double layer capacitance, H adsorption, oxide stripping) to determine electroactive surface area

H_I-ePt
0.008 cm^2
200 mV s^{-1}
2 M H_2SO_4
25 ° C

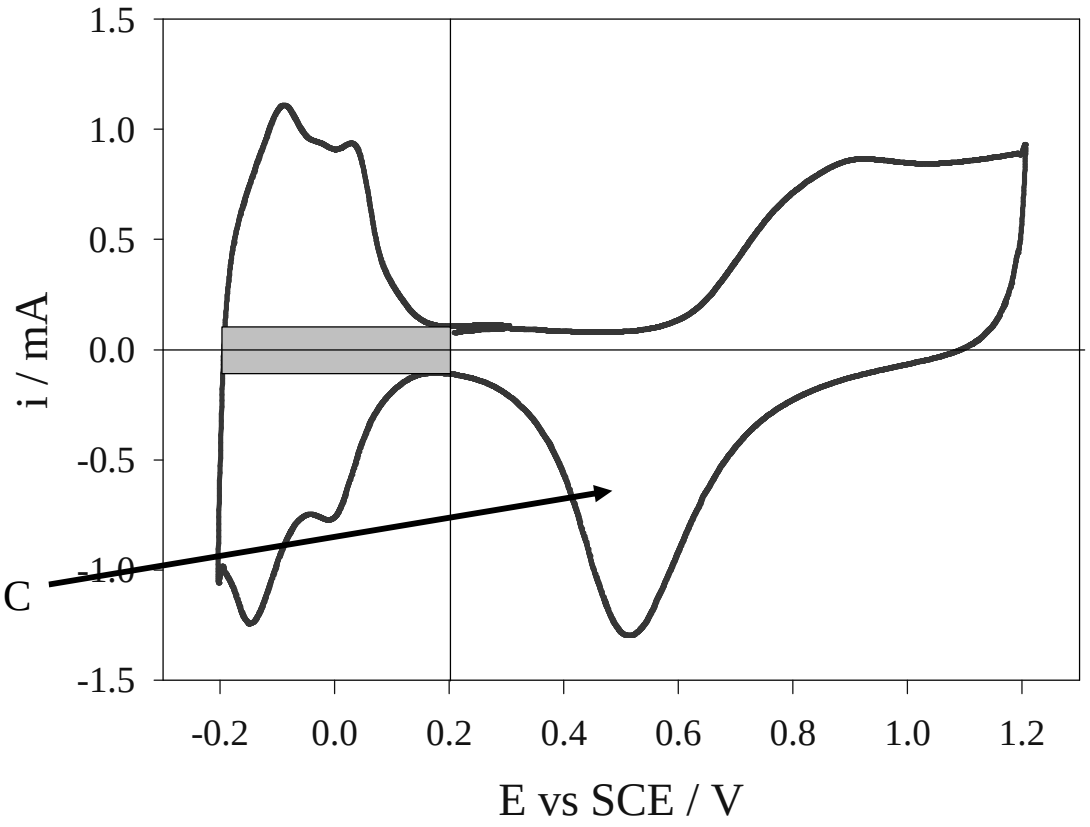

$$Q = \frac{1}{2} \times \frac{600\ \text{mV}}{200\ \text{mV s}^{-1}} \times 1.3\ \text{mA} = 3.9\ \text{mC}$$

Pt oxide stripping is 233 μC cm^{-2}

active surface area is ~ 16.7 cm^2 → roughness ~ 2000

Control over structure

- $C_{12}EO_8$

  17.5 ± 2 Å pores

- $C_{16}EO_8$

  25 ± 1.5 Å pores

- $C_{16}EO_8$/heptane (2:1)

  35 ± 1.5 Å pores

G. S. Attard, P. N. Bartlett, N. R. B. Coleman, J. M. Elliott, J. R. Owen, and J. H. Wang, “Nanostructured platinum films from lyotropic liquid crystalline phases”, *Science*, **278**(1997)838-840.

Ia3d-ePt

Cubic V_I

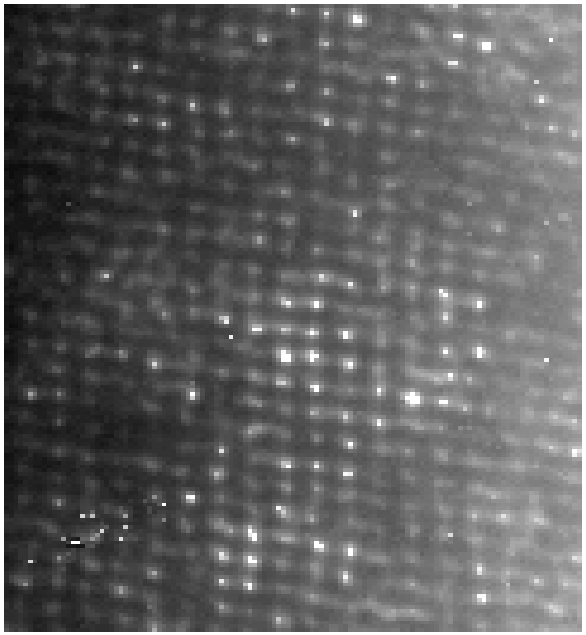

50 nm

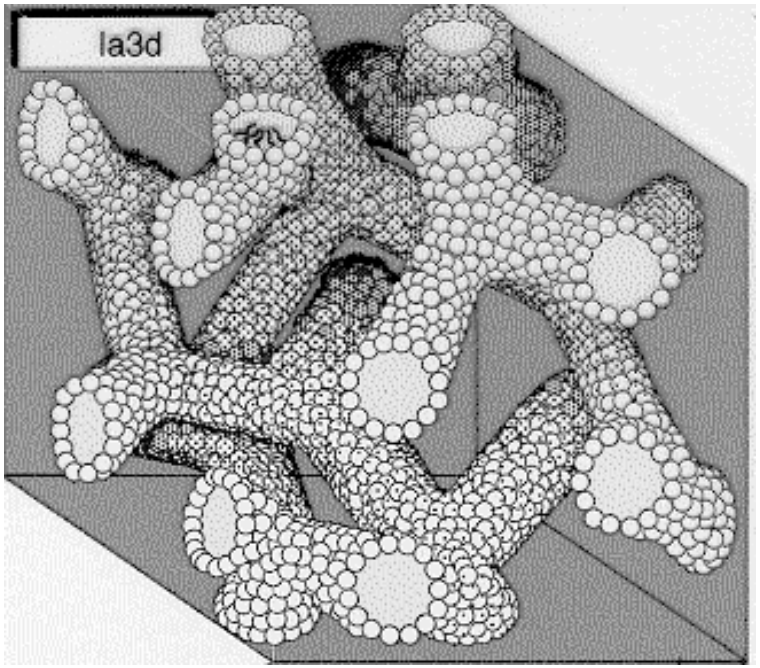

J. M. Elliott, G. S. Attard, P. N. Bartlett, N. R. B. Coleman, D. A. S. Merckel and J. R. Owen, “Nanostructured platinum (H_I-ePt) films: Effects of electrodeposition conditions on film properties”, *Chem. Mater.*, **11** 1999, 3602-3609.

Examples of applications:

As electrode for O_2 reduction

P. R. Birkin, J. M. Elliott and Y. E. Watson, “Electrochemical reduction of oxygen on mesoporous platinum microelectrodes”, *Chem. Commun*, 2000, 1693-4.

As electrode for H_2O_2 electrochemistry

S. A. G. Evans, J. M. Elliott, L. M. Andrews, P. N. Bartlett, P. J. Doyle and G. Deunault, “Detection of hydrogen peroxide at mesoporous platinum microelectrodes”, *Anal. Chem*., **74,** 2002, 1322-1326.

For use in batteries

A. H. Whitehead, J. M. Elliott, and J.R Owen, “Nanostructured tin for use as a negative electrode material in Li-ion batteries”, *J. Power Sources*, **81-82,** 1999, 33-8.

For use as catalyst in MeOH fuel cell

J. Jiang and A. Kucernak, “Electrooxidation of small organic molecules on mesoporous precious metal catalysts II: CO and methanol on platinum-ruthenium alloy”, *J Electroanal. Chem*., **543**, 2003, 187-199.

Catalyst for gas sensor

P. N. Bartlett and S. Guerin, “A micromachined calorimetric gas sensor: An application of electrodeposited nanostructured palladium for the detection of combustible gases”, *Anal. Chem.*, **75**, 2003, 126-132.

Planar Pellistor

H_1-e Pd used as a catalyst on a micromachined planar methane sensor

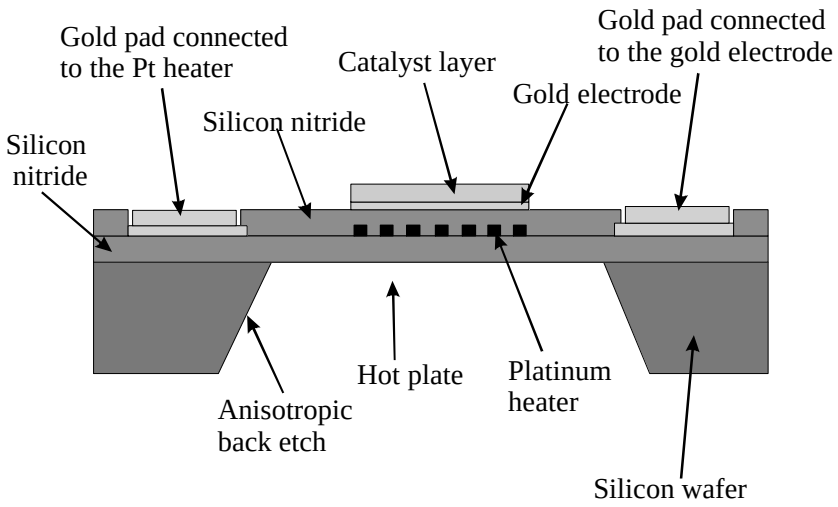

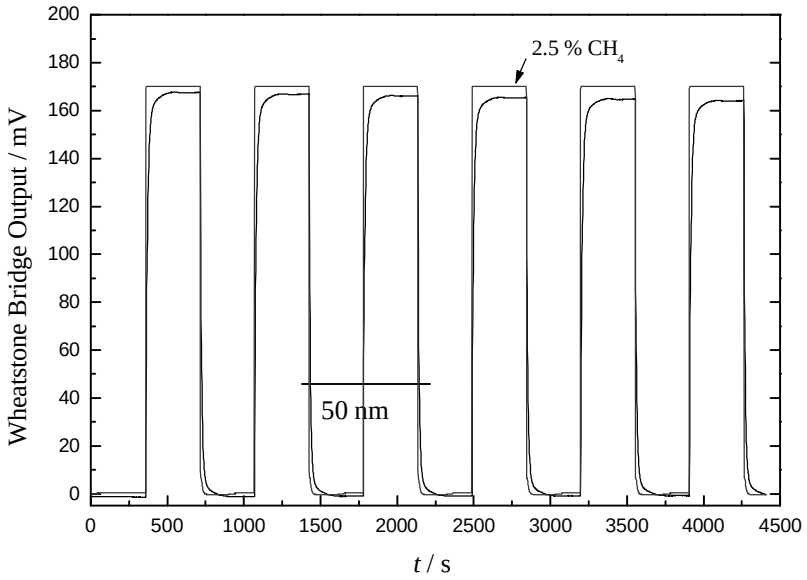

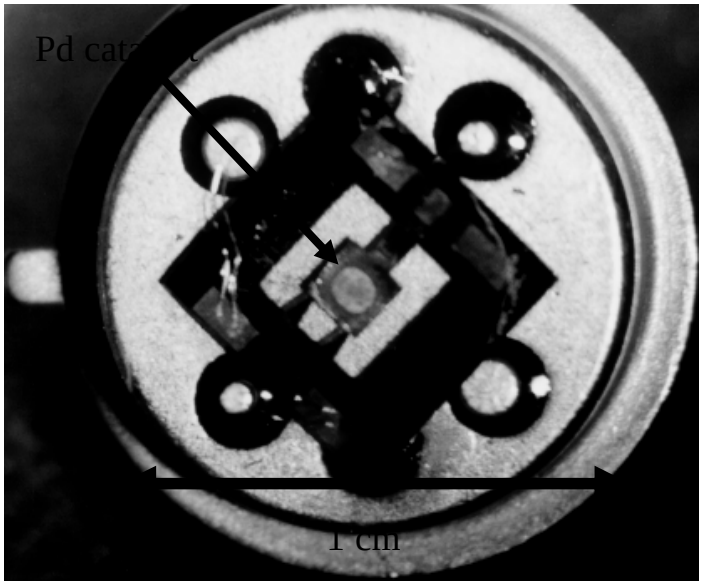

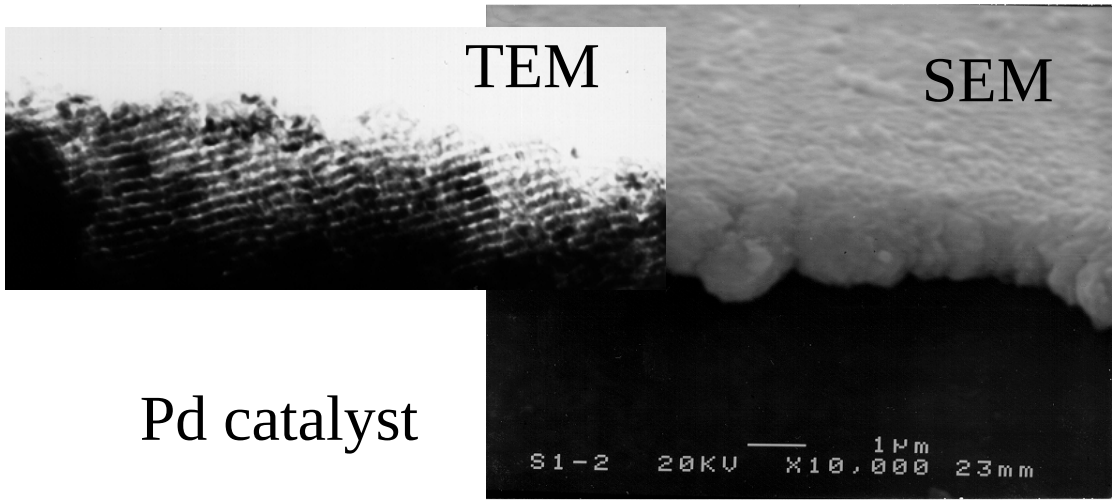

Pd catalyst

Mesostructured films (20-1000 nm)

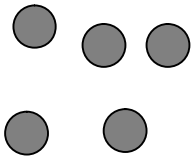

Uniform poly(styrene) latex particles 20-1000 nm diameter

Assemble template

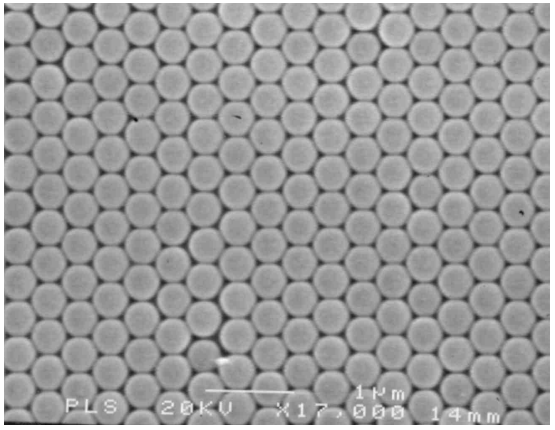

Electroplate metal

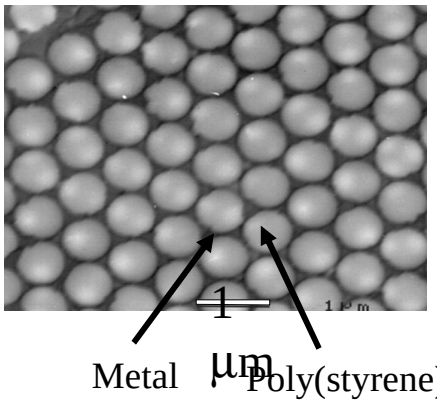

Remove template

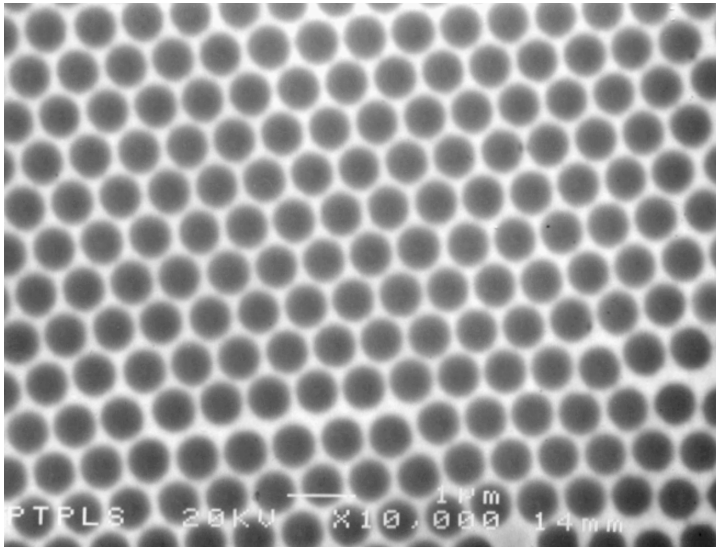

Platinum film, deposition charge -1.20 C cm^{-2}, polystyrene latex sphere diameter 0.70 μm.

P. N. Bartlett, P. R. Birkin and M. A. Ghanem, “Electrochemical deposition of macroporous platinum, palladium and cobalt films using polystyrene latex sphere templates”, *J. Chem. Soc. Chem. Commun.*, 2000, 1671-1672.

Assembly of the Template

Solution of Colloidal Spheres

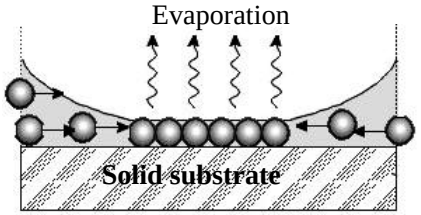

Via attractive capillary forces

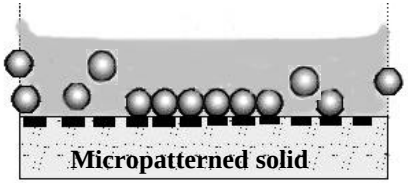

Micropatterned substrate via sedimentation

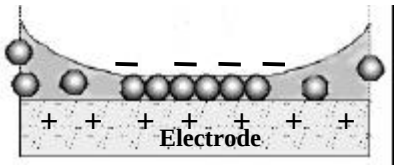

Electrophoretic deposition

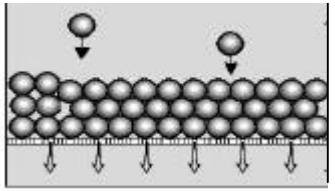

Filtration

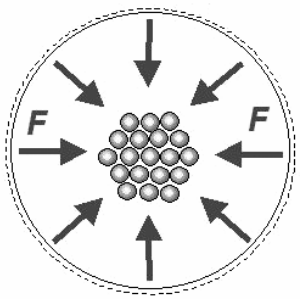

Water flux
force direction

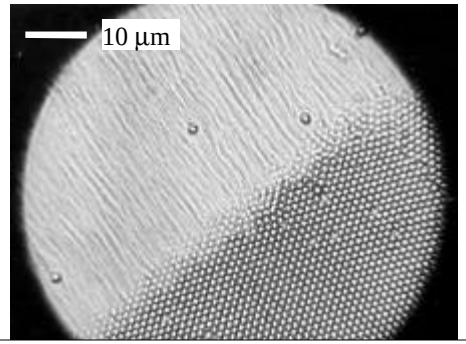

Optical microscope image for the 2D ordering process for colloidal spheres

Nagayama *et al.*, *Langmuir*, **15**, 5257(1999).

Advantages of electrodeposition

- it is a volume templating method
- no shrinkage of the material when the template is removed
- no further processing steps or use of high *T*
- diameter of voids is directly determined by diameter template spheres, *d*
- wide choice of materials
- control over film thickness, *t*
- produces thin supported layers
- different surface topography for $t < d$ and $t > d$
- for $t > d$ surface topography is modulated in a regular manner that depends on the deposition conditions.

Evolution of surface topography

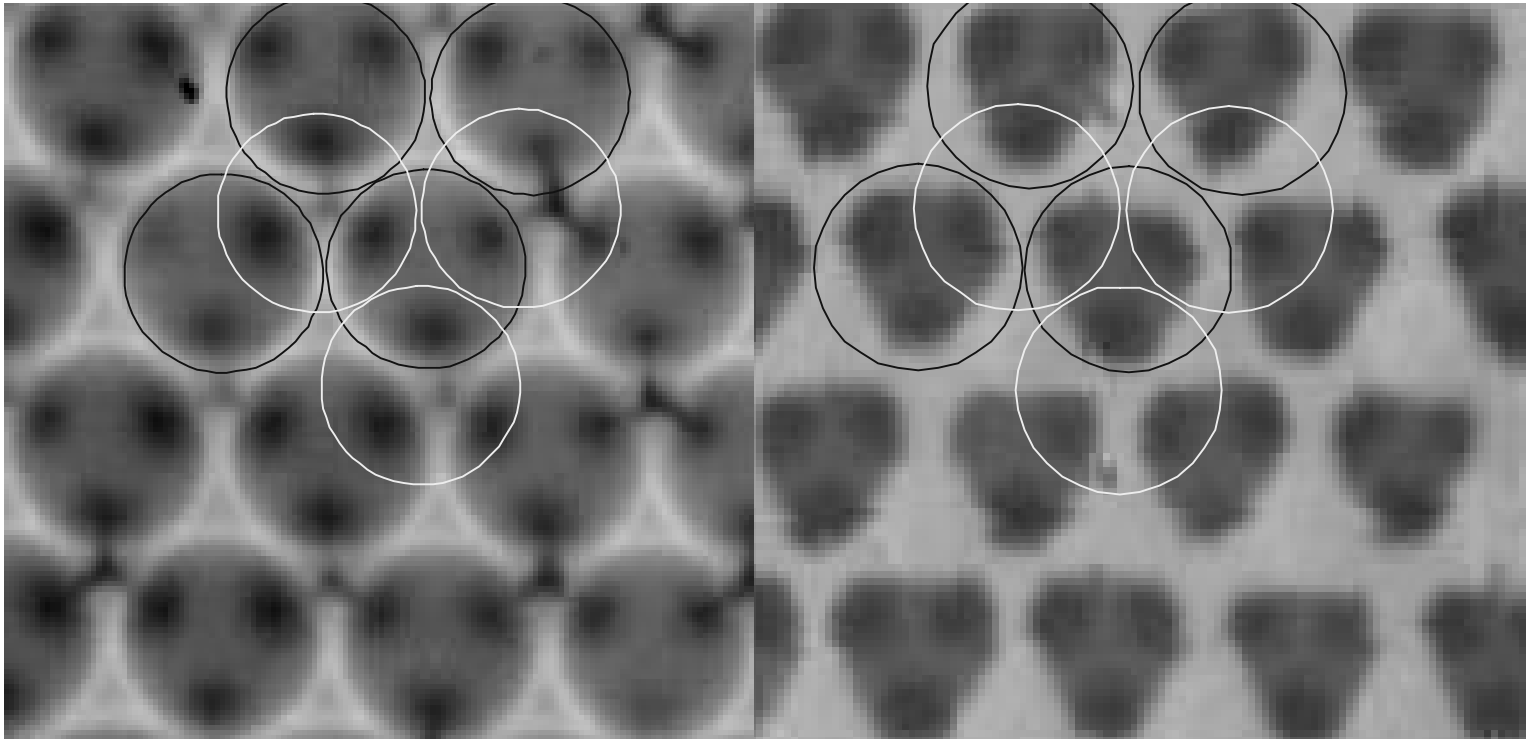

$t/d \sim 1.5$ $t/d \sim 1.7$

P. N. Bartlett, J. J. Baumberg, P. R. Birkin, M. A. Ghanem and M. C. Netti, “Highly Ordered Macroporous Gold and Platinum Films formed by Electrochemical Deposition through Templates Assembled from Submicron Diameter Monodisperse Polystyrene Spheres” *Chem. Mater.*, **14**, 2002, 2199-2208.

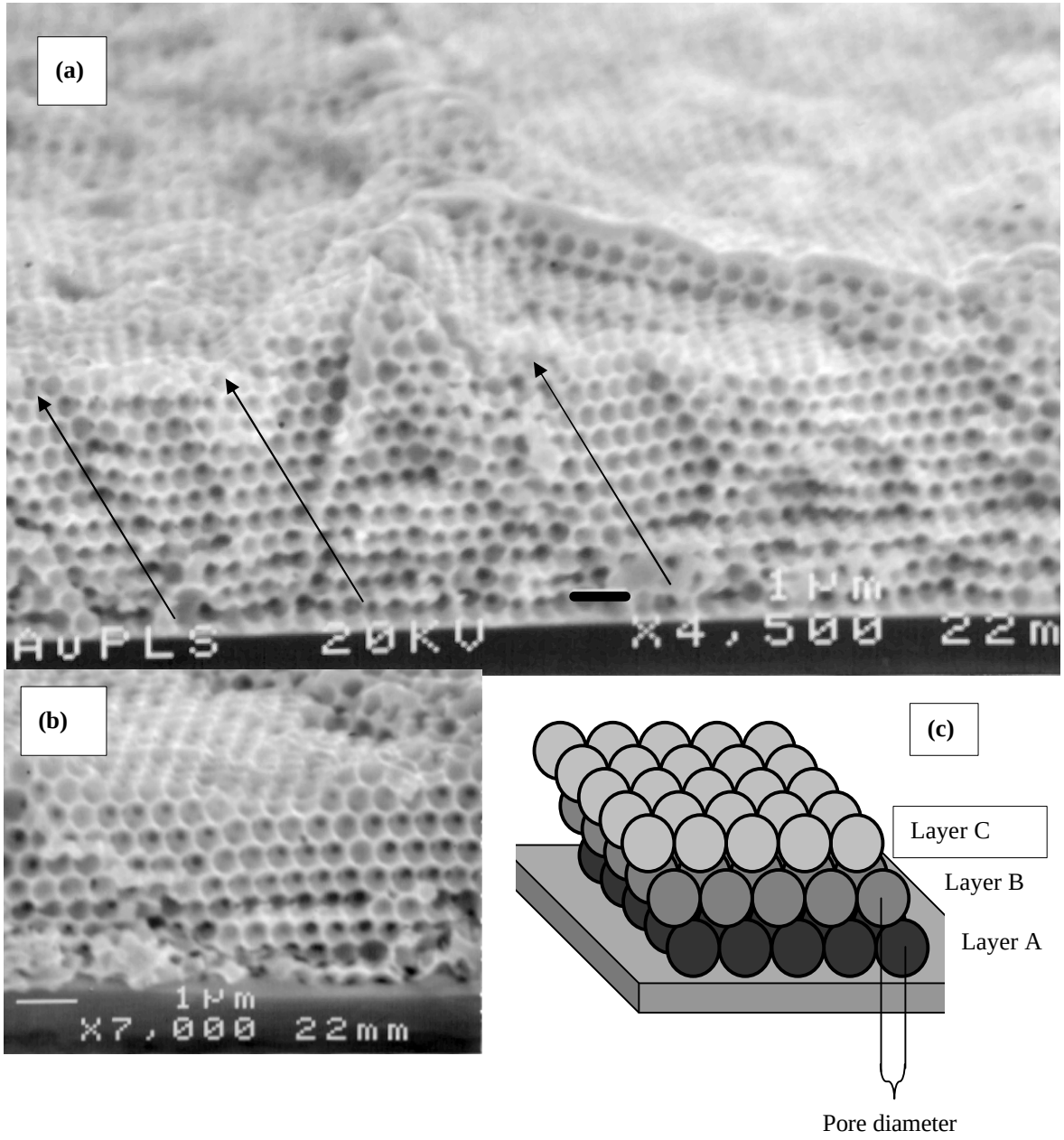

Template assembled form 500 nm diameter polystyrene spheres, total deposition charge passed 2.80 C cm^{-2}. Scale bar 1.0 µm.

Nanostructured Pt

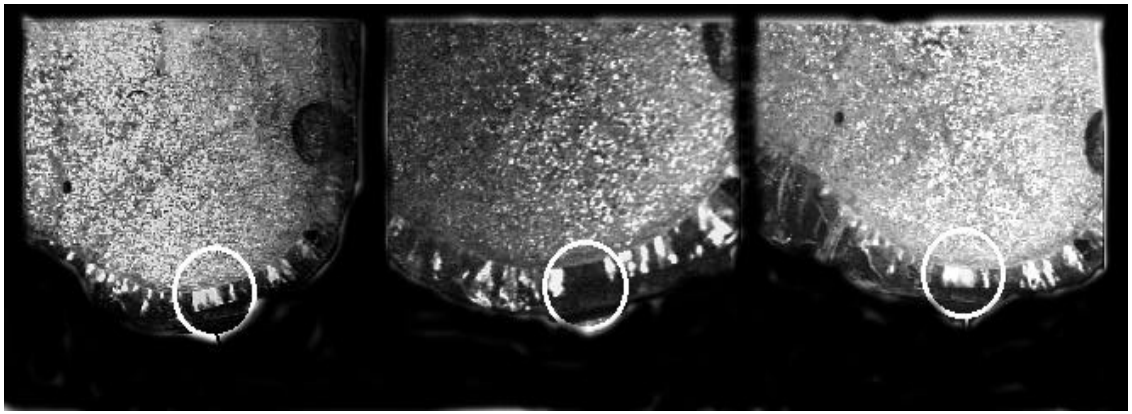

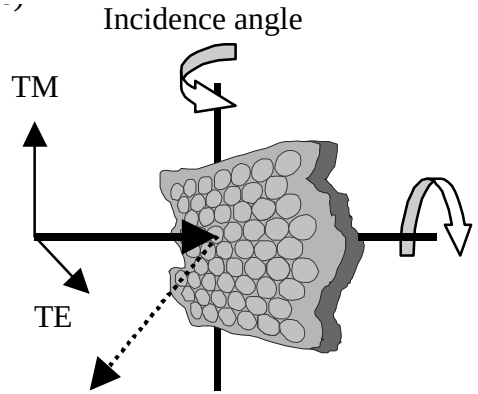

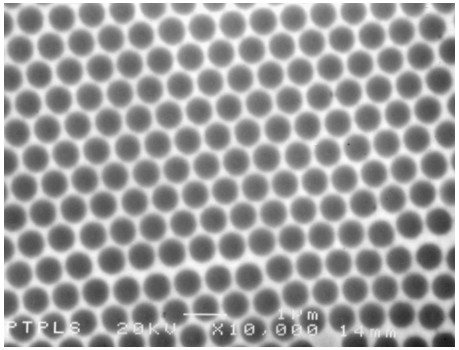

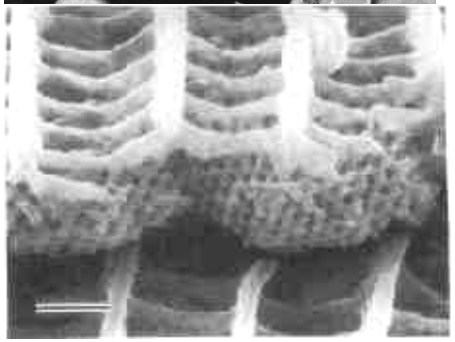

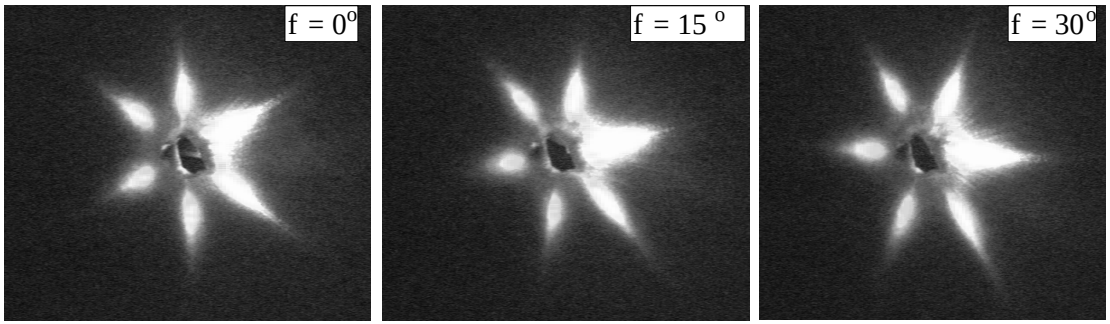

Chem. Mater., **14**, 2002, 2199.

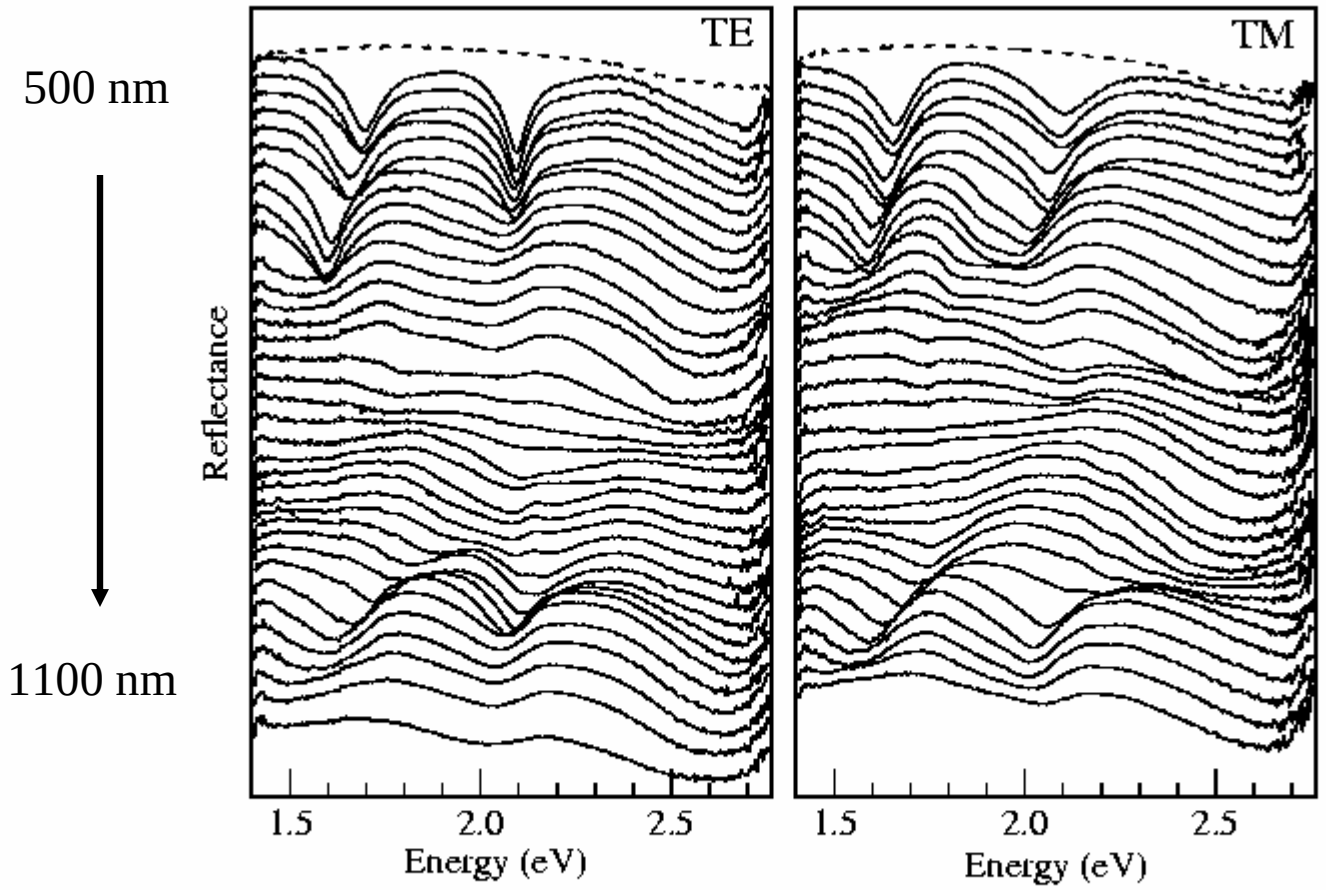

Narrow (< 20 nm half width), intense (> 100x) resonances at certain thicknesses

Reflectivity spectra at different thicknesses (500-1100 nm from top to bottom) for both TE and TM polarised incident light at 45°. The scale is logarithmic and the curves have been offset for clarity. The dotted curve is an unpatterned film electrodeposited under the same conditions.

Reflectance spectra for Au samples

- spectra are insensitive to azimuthal angle
- changes in angle of incidence alter relative intensity but not position of resonances
- effect is not seen for Co or Pt

Conclude that effect is due to localised plasmon-polariton

Magnetic properties

Putting arrays of uniform sub-micron pores into magnetic materials alters their magnetic properties.

This happens both at 1 nm and 100 nm scales.

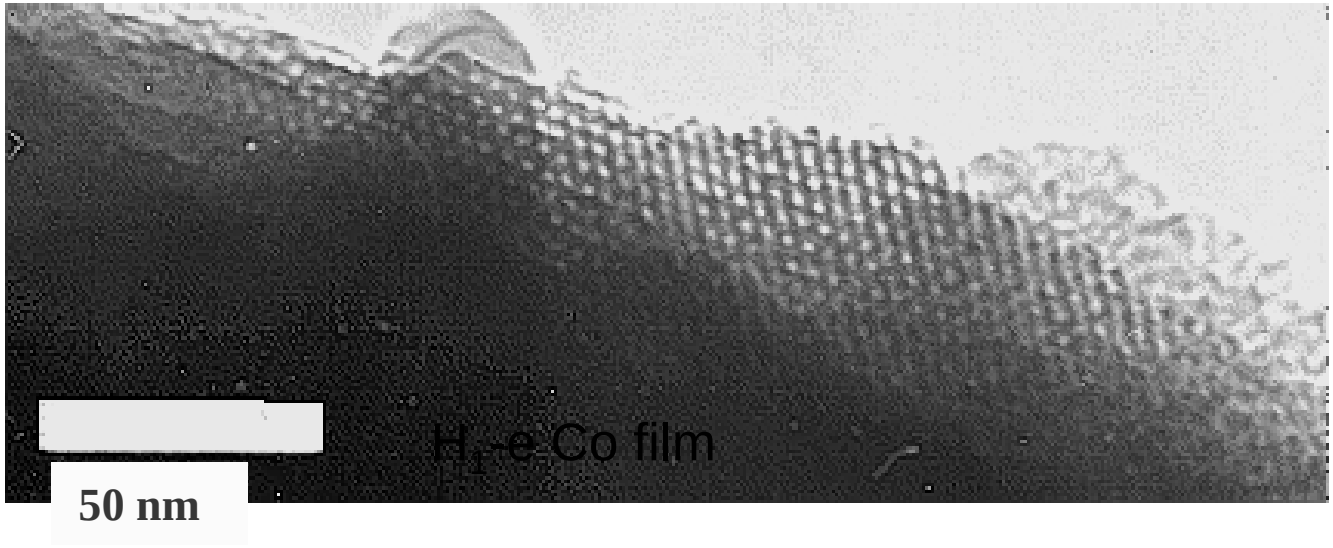

P. N. Bartlett, P. R. Birkin, M. A. Ghanem, P. de Groot and M. Sawicki, “The electrochemical deposition of nanostructured cobalt films from lyotropic liquid crystalline media”, *J. Electrochem. Soc.*, **148**, 2001, C119-C123.

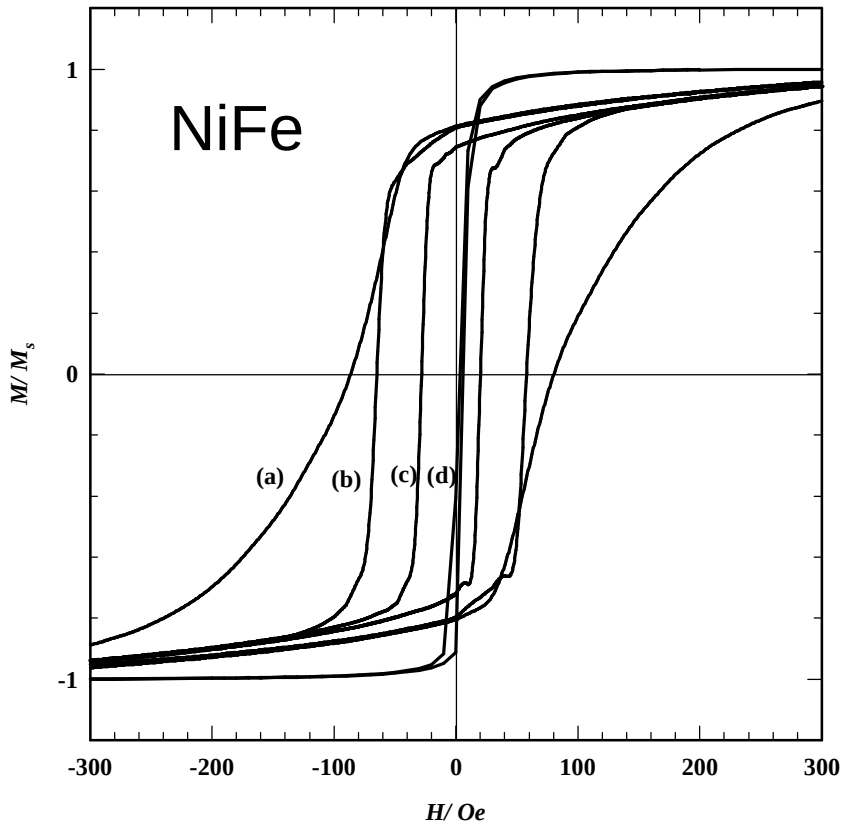

Macroporous NiFe

d (nm)	H_c (Oe)
0.0	1.50
1000	20.0
750	55.0
500	58.0
200	81.0

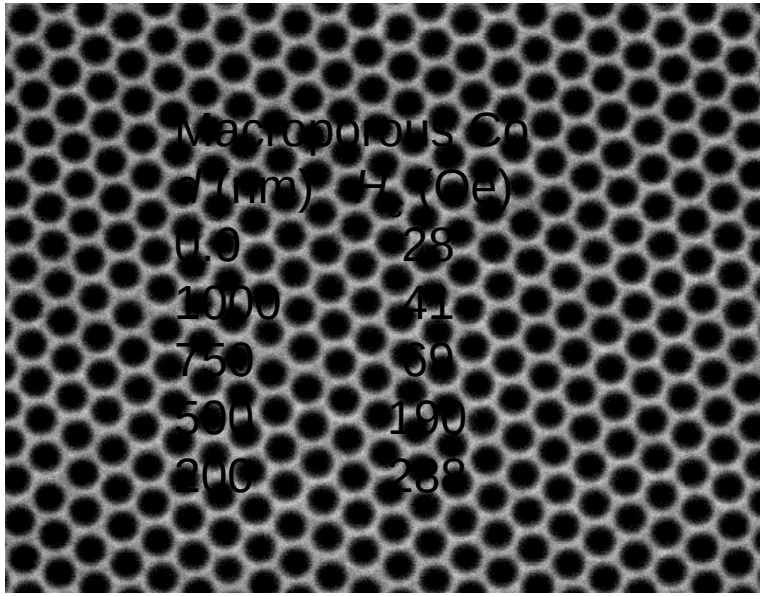

The normalised in-plain magnetization curves measured at room temperature for electrochemically deposited macroporous NiFe alloy films using (a) 0.20, (b) 0.50, and (c) 1.00 μm polystyrene sphere templates. The plain NiFe alloy film (d) is shown for comparison. All films were 0.50 μm thick as measured by SEM.

Magnetic properties of nanostructured films vary with pore diameter and geometry

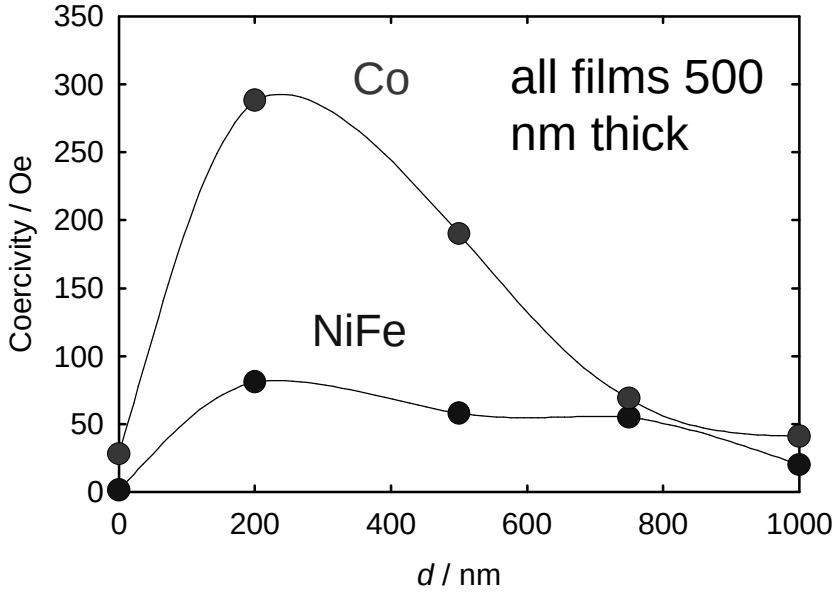

vary pore size

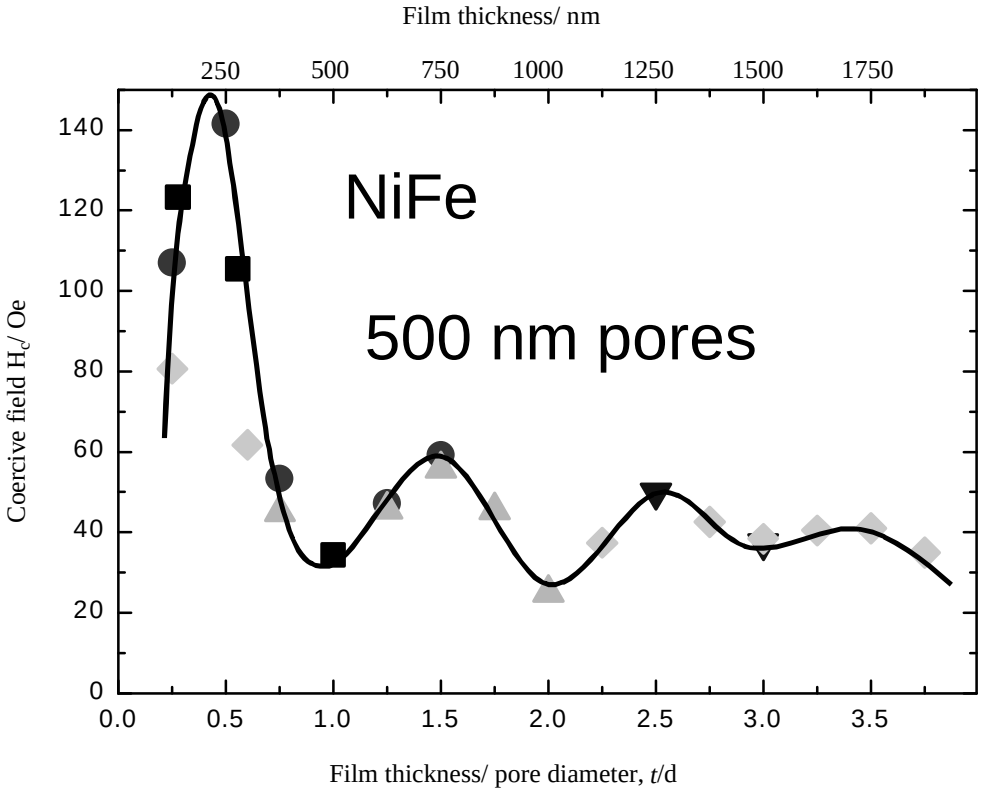

vary film thickness

A. A. Zhukov, A. V. Goncharov, P. A. J. de Groot, M. A. Ghanem, I. S. El-Hallag and P. N. Bartlett, "Coercivity of 3D nanoscale magnetic arrays from self-assembly template methods", *J. Magnetism and Magnetic Materials*, submitted.
P. N. Bartlett, M. A. Ghanem, I. S. El Hallag, P. de Groot, A. Zhukov, "Electrochemical Deposition of Macroporous Magnetic Networks using Colloidal Templates", *J. Mater. Chem.*, submitted.

$$Pb^{2+} + 2H_2O \rightarrow PbO_2 + 4H^+ + 2e$$

0.1 M $Pb(NO_3)_2$, 1 M HNO_3

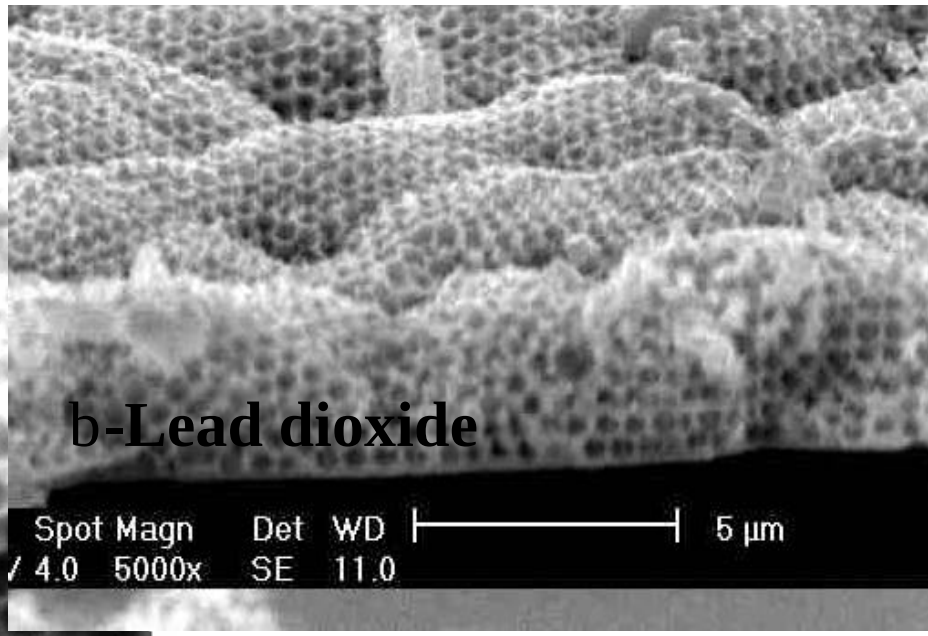

0.1 M $Pb(OAc)_2$, 1 M NaOAc

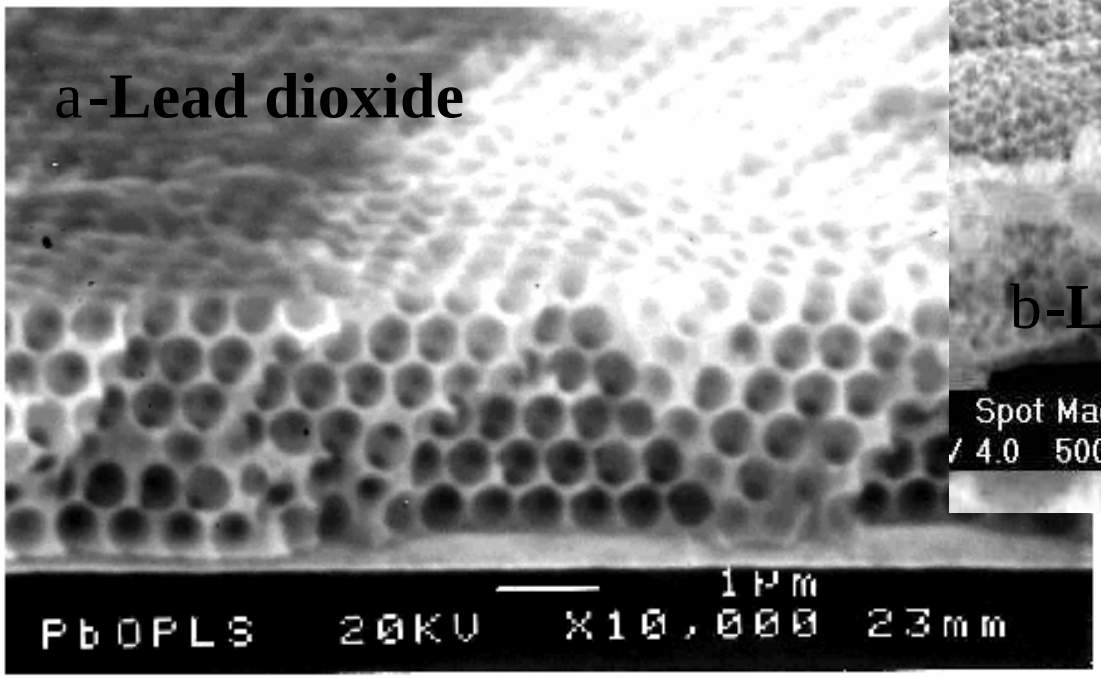

P. N. Bartlett, T. Dunford and M. A. Ghanem, "Templated electrochemical deposition of nanostructured macroporous PbO_2", *J. Mater. Chem.*, **12,** 2002, 3130-3135.

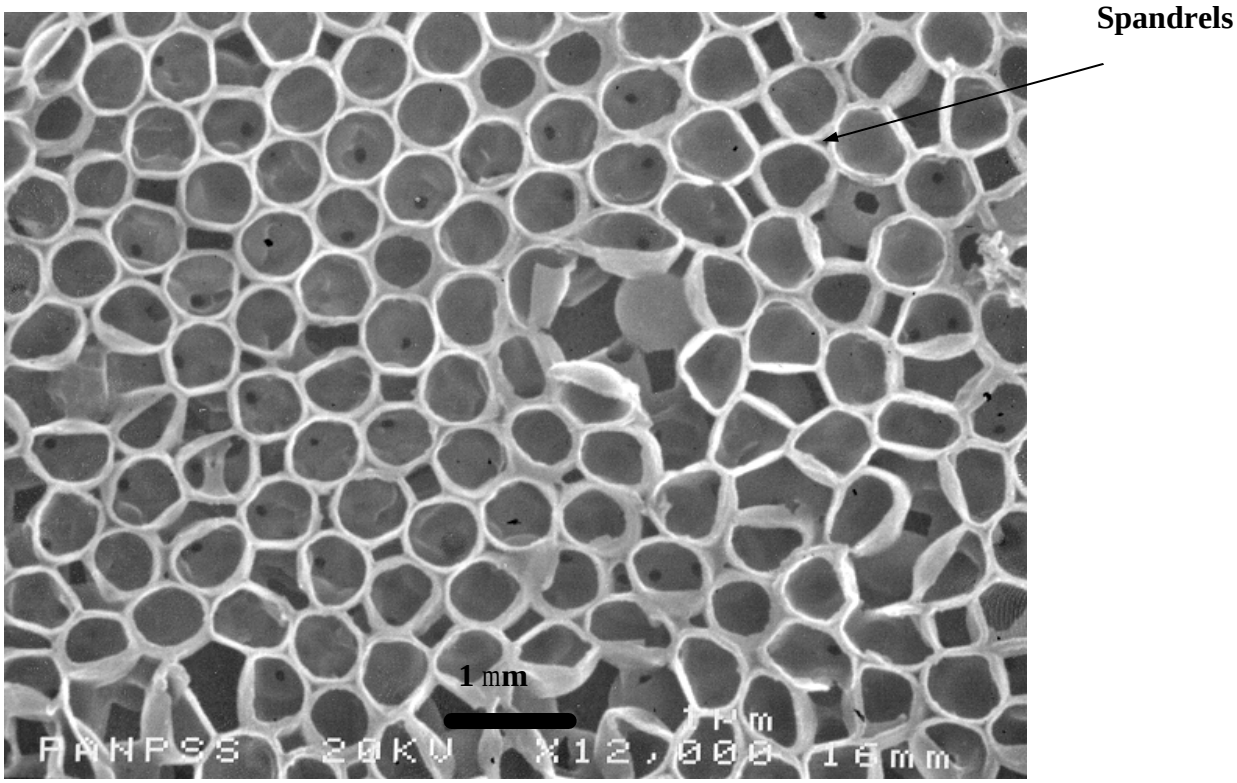

Macroporous poly(aniline)/poly(vinylsulfonate) (750 nm sphere template), film thickness approximately three times the sphere diameter; deposition charge = 59 mC/cm^2.

P. N. Bartlett, P. R. Birkin, M. A. Ghanem and C-S. Toh, “Electrochemical syntheses of highly ordered macroporous conducting polymers using self-assembled colloidal templates”, *J. Materials Chem.*, **11**, 2001, 849-853.

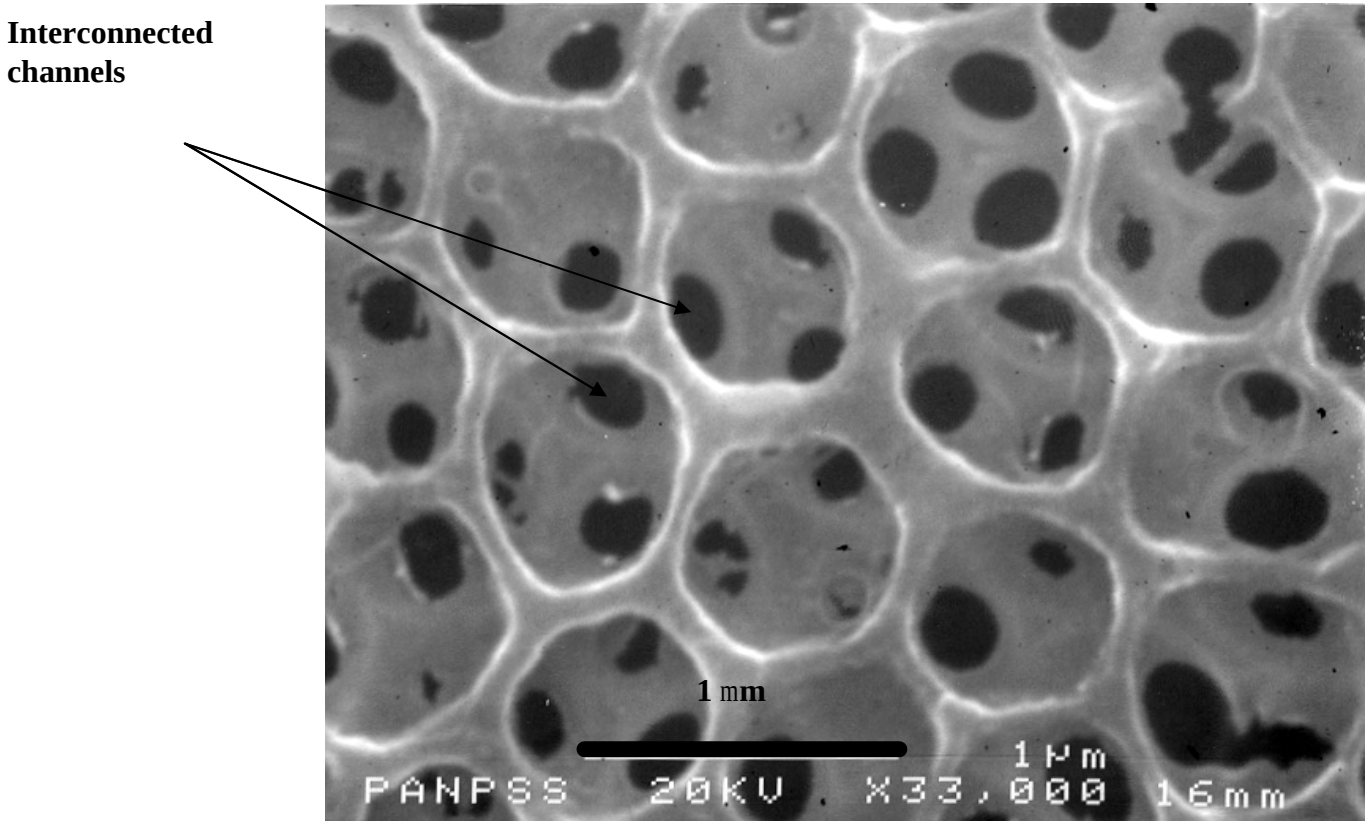

Macroporous poly(aniline)/poly(styrenesulfonate) (750 nm sphere template) showing interconnected channels; deposition charge = 31 mC/cm^2.

Further Reading

D. Pletcher, *A First Course in Electrode Processes*, The Electrochemical Consultancy (Romsey) , 1991.

P.H. Reiger, *Electrochemistry*, Prentice-Hall, 1987.

M. Paunovic and M. Schlessinger, *Fundamentals of Electrochemical Deposition*, Wiley, 1998.

M. Paunovic and M. Schlessinger, *Modern Electroplating*, 4th Edn., Wiley, 2000.